https://doi.org/10.1093/plcell/koac241 THE PLANT CELL 2022: 34: 4453–4471

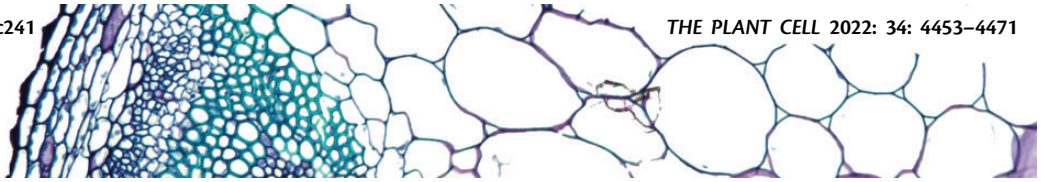

Research Article

HPCA1 is required for systemic reactive oxygen species and calcium cell-to-cell signaling and plant acclimation to stress

Yosef Fichman [1], Sara I. Zandalinas [2], Scott Peck [3], Sheng Luan [4] and Ron Mittler [1,5,*]

1 Division of Plant Sciences and Technology, College of Agriculture Food and Natural Resources and Interdisciplinary Plant Group, University of Missouri, Columbia, Missouri 65211, USA
2 Department of Agricultural and Environmental Sciences, University Jaume I, Castelló de la Plana, 12071, Spain
3 Department of Biochemistry, College of Agriculture Food and Natural Resources and Interdisciplinary Plant Group, University of Missouri, Columbia, Missouri 65211, USA
4 Department of Plant and Microbial Biology, University of California, Berkeley, California 94720, USA
5 Department of Surgery, University of Missouri School of Medicine, Christopher S. Bond Life Sciences Center, University of Missouri, Columbia, Missouri 65201, USA

*Author for correspondence: mittlerr@missouri.edu

Conceptualization: R.M., Y.F., S.I.Z.; Investigation: Y.F., S.I.Z.; Visualization: Y.F., S.I.Z.; Funding acquisition: R.M.; Resources: S.L., S.P., R.M.; Writing – original draft: R.M., Y.F.; Writing – review and editing: R.M., Y.F., S.I.Z., S.L., S.P.
The author(s) responsible for distribution of materials integral to the findings presented in this article in accordance with the policy described in the Instructions for Authors (https://academic.oup.com/plcell) is Ron Mittler (mittlerr@missouri.edu)

Abstract

Reactive oxygen species (ROS), produced by respiratory burst oxidase homologs (RBOHs) at the apoplast, play a key role in local and systemic cell-to-cell signaling, required for plant acclimation to stress. Here we reveal that the *Arabidopsis thaliana* leucine-rich-repeat receptor-like kinase H_2O_2-INDUCED CA^{2+} INCREASES 1 (HPCA1) acts as a central ROS receptor required for the propagation of cell-to-cell ROS signals, systemic signaling in response to different biotic and abiotic stresses, stress responses at the local and systemic tissues, and plant acclimation to stress, following a local treatment of high light (HL) stress. We further report that HPCA1 is required for systemic calcium signals, but not systemic membrane depolarization responses, and identify the calcium-permeable channel MECHANOSENSITIVE ION CHANNEL LIKE 3, CALCINEURIN B-LIKE CALCIUM SENSOR 4 (CBL4), CBL4-INTERACTING PROTEIN KINASE 26 and Sucrose-non-fermenting-1-related Protein Kinase 2.6/OPEN STOMATA 1 (OST1) as required for the propagation of cell-to-cell ROS signals. In addition, we identify serine residues S343 and S347 of RBOHD (the putative targets of OST1) as playing a key role in cell-to-cell ROS signaling in response to a local application of HL stress. Our findings reveal that HPCA1 plays a key role in mediating and coordinating systemic cell-to-cell ROS and calcium signals required for plant acclimation to stress.

Introduction

Reactive oxygen species (ROS; i.e. H_2O_2, O_2^-, $^1O_2$, and $HO^{\cdot}$) are credited with playing a fundamental role in the evolution of life on Earth, impacting processes such as endosymbiotic events, the emergence of multicellularity, and the development of sexual reproduction (Gutteridge and Halliwell, 2018; Hörandl and Speijer, 2018; Taverne et al.,

Received June 24, 2022. Accepted July 16, 2022. Advance access publication August 4, 2022

IN A NUTSHELL

Background: Plants grow and reproduce in a highly dynamic environment that can change abruptly. To adjust to changes in their environment, the different cells of a plant communicate with each other exchanging signals that coordinate responses to the environment between different parts and tissues of the plant. The different signals plant cells exchange with each other include hormones, electric signals, hydraulic pressure signals, and calcium and ROS signals/waves. The ability of plant cells to communicate with each other plays a key role in plant acclimation to different environments and overall survival during stress.

Question: Although the different signals exchanged by plant cells have been studied, how they are linked with each other and how ROS and calcium regulate each other are largely unanswered questions.

Findings: Our study identified the plant receptor required for the exchange of ROS signals between cells. This receptor was also found to be a key player in linking ROS and calcium signals (but not electric signals) during responses to light stress. Studying different mutants deficient in mediating cell-to-cell ROS signals we also identified the signal transduction cascade that links the ROS receptor with the enzyme that produces ROS on the extracellular side of the plant plasma membrane. Our work therefore dissected the reactive oxygen-induced-reactive oxygen-release cell-to-cell signal transduction pathway of the plant that is also known as "the ROS wave".

Next steps: One of the most important next steps is to determine how the ROS receptor regulates calcium signals. We identified a putative calcium-permeable channel involved in this pathway, but the protein–protein interactions and mode of regulation of this (or other) calcium-permeable channel by the receptor remains to be determined.

2018; Jabłońska and Tawfik, 2021). Although originally considered to be toxic byproducts of aerobic metabolism, in recent years, numerous studies revealed that ROS, such as H_2O_2 and $O_2^{\cdot-}$, are essential for life, acting as key regulators of redox, stress responses, and cell-to-cell signaling (Schieber and Chandel, 2014; Mittler, 2017; Sies and Jones, 2020; Mittler et al., 2022). Examples of the roles of ROS in cell-to-cell signaling include the recruitment of macrophages to wound sites and interactions between neurons in animals, communication between microorganisms within a microbiome, and transmission of long-distance cell-to-cell signals in plants (Aguirre and Lambeth, 2010; Razzell et al., 2013; Zheng et al., 2015; Zandalinas et al., 2020a, 2020b; Fichman et al., 2021; Iwashita et al., 2021).

In the flowering plant *A. thaliana* (Arabidopsis), cell-to-cell ROS signaling plays a pivotal role in local and systemic responses, acclimation, and survival of plants during stress (Mittler et al., 2011, 2022; Zhu, 2016; Waszczak et al., 2018; Smirnoff and Arnaud, 2019; Zandalinas et al., 2020a, 2020b; Fichman et al., 2021). During this process, ROS production is triggered in cells directly subjected to stress (termed "local tissue"), and a state of activated ROS production, driven by the function of respiratory burst oxidase homologs (RBOHs), the plant equivalents of mammalian NADPH oxidases, is propagated from cell-to-cell over long distances, sometime spanning the entire length of the plant (Mittler et al., 2011, 2022; Zhu, 2016; Fichman et al., 2019, 2021; Zandalinas et al., 2020a, 2020b; Fichman and Mittler, 2020b). Once the activated ROS production state reaches cells and tissues other than the ones initiating it (i.e. tissues not directly subjected to stress; termed "systemic tissues"), it activates in them different acclimation mechanisms and enhances the overall resilience of the plant to stress (termed "systemic acquired acclimation"; SAA; Karpinski et al., 1999; Zandalinas et al., 2020a, 2020b; Fichman et al., 2021).

Although cell-to-cell ROS signaling (termed the "ROS wave") is essential for systemic signaling and SAA to occur, it does not convey specificity to the systemic response and is therefore linked with other, yet unknown, stress-specific systemic signals, as well as with cell-to-cell calcium and membrane potential signaling processes (Suzuki et al., 2013; Fichman and Mittler, 2020a, 2021a; Fichman et al., 2021). While RBOHs such as RBOHD and RBOHF produce apoplastic ROS essential for this process (Miller et al., 2009, Mittler et al., 2022; Fichman et al., 2019, 2021; Zandalinas et al., 2020a, 2020b; Fichman and Mittler, 2020b), the identity of the ROS receptor(s) perceiving the apoplastic ROS signal and enabling the cell-to-cell ROS signaling process to occur is currently unknown.

We recently developed a method for whole-plant live ROS imaging to visualize cell-to-cell ROS signaling in mature plants growing in soil (Fichman et al., 2019; Fichman and Mittler, 2020b). Using this method, we screened over 120 different mutants, potentially involved in ROS and calcium signaling, for the presence or absence of the ROS wave in response to a local treatment of high light (HL) stress (Supplemental Data Set 1). Among the different mutants we screened were those affecting several putative receptors, including different cysteine-rich receptor-like kinases (CRKs) and the leucine-rich-repeat receptor-like kinase (LRR-RLK), H_2O_2-INDUCED CA^{2+} INCREASES 1 (HPCA1; At5g49760), also known as CANNOT RESPOND TO DMBQ 1 (CARD1).

HPCA1/CARD1 was recently identified as a receptor for extracellular H_2O_2 (Wu et al., 2020), as well as a sensor for

the oxidizing molecule quinone (Laohavisit et al., 2020). Here we reveal that HPCA1 acts as a key ROS receptor required for the accumulation of ROS in stressed tissues, propagation of cell-to-cell ROS signals, systemic signaling in response to different biotic and abiotic stresses, and plant acclimation to stress. We further show that HPCA1 is required for systemic calcium signals (also termed the "calcium wave"), but not for systemic membrane depolarization responses (a type of "electric wave"), and that systemic calcium signals mediated by HPCA1 require the function of the calcium-permeable channel MECHANOSENSITIVE ION CHANNEL LIKE 3 (MSL3). In addition, we reveal that key components of calcium-dependent signaling cascades, such as the CALCINEURIN B-LIKE CALCIUM SENSOR (CBL4; also known as SOS3), the CBL4-INTERACTING PROTEIN KINASE 26 (CIPK26), and Sucrose-non-fermenting-1-Related Protein Kinase 2.6 (SnRK2.6), also termed OPEN STOMATA 1 (OST1), are involved in this process. We further identify serine residues S343 and S347 of RBOHD (the putative targets of OST1) as playing a key role in cell-to-cell ROS signaling in response to a local application of HL stress. Our findings reveal that HPCA1 plays a key role in the sensing of H_2O_2 produced at the apoplast during cell-to-cell signaling, linking the accumulation of apoplastic H_2O_2 with calcium cascades and the activation of further ROS production by RBOHs, thereby mediating and coordinating systemic cell-to-cell ROS and calcium signals that are required for plant resilience to stress.

Results

HPCA1 is required for systemic cell-to-cell ROS and calcium signaling during plant responses to HL stress

To study the role of HPCA1 in systemic cell-to-cell ROS signaling, we subjected a single leaf of wild-type (WT) and two independent knockout alleles of HPCA1 (*hpca1-1*, *hpca1-2*) to a HL stress treatment of 1,700 µmol photons $s^{-1}m^{-2}$ for 2 min and used our newly developed whole-plant live ROS imaging method with 2′,7′-dichlorodihydrofluorescein diacetate (H_2DCFDA) as a probe (Fichman et al., 2019) to measure the accumulation of ROS in local and systemic leaves over a period of 30 min. HL stress can occur in shaded plants or shaded canopy leaves as a result of sunflecks, or in field grown plants when the sunlight is intermittently blocked by clouds (Karpinski et al., 1999; Kromdijk et al., 2016; Slattery et al., 2018). As shown in Figure 1A, mutants deficient in HPCA1 (*hpca1-1*, *hpca1-2*) did not accumulate ROS in their local or systemic leaves in response to a local application of HL stress (see also Movie 1). Because H_2DCFDA detects a broad range of different ROS, we also used Peroxy Orange 1 (PO1; Fichman et al., 2019) instead of H_2DCFDA as a probe, to measure the levels of H_2O_2 that accumulate in local and systemic leaves of WT, *hpca1-1*, and *hpca1-2* plants following a similar HL treatment. As shown in Figure 1B, H_2O_2 accumulated in local and systemic leaves of WT, but not the *hpca1-1* and *hpca1-2* mutants in response to a local treatment of HL stress. Similar results were also observed in extracts obtained from treated and untreated local and systemic leaves of WT, *hpca1-1*, and *hpca1-2* plants when the levels of H_2O_2 were quantified using the Amplex-Red method (Figure 1C).

Upon sensing of H_2O_2, HPCA1 was found to trigger the accumulation of calcium in the cytosol (Wu et al., 2020). This process could activate another type of cell-to-cell signaling pathway termed the "calcium wave", which is dependent on the function of the calcium channels GLUTAMATE-LIKE RECEPTOR 3.3 and 3.6 (GLR3.3 and GLR3.6) (Evans et al., 2016; Toyota et al., 2018; Shao et al., 2020; Fichman and Mittler, 2021a). To determine whether HPCA1 is also required for systemic cell-to-cell calcium signals, we subjected a single leaf of WT, *hpca1-1*, and *hpca1-2* plants to the same HL stress treatment described above and used Fluo-4-AM as a probe in our live imaging platform (Fichman and Mittler, 2021a) to measure changes in cytosolic calcium levels in local and systemic leaves over a period of 30 min. As shown in Figure 2A, mutants deficient in HPCA1 (*hpca1-1*, *hpca1-2*) did not display local or systemic changes in cytosolic calcium levels in response to a local application of HL stress (see also Movie 1). Interestingly, the HL-induced local and systemic calcium signal observed in WT plants was not transient (Figure 2; Movie 1). This finding agrees with our previous findings (Fichman and Mittler 2021a) and the work of Toyota et al., (2018), and corresponds with the elevated levels of local and systemic ROS that persist for about 3- to 6-h post a 2- or 10-min HL stress treatment of a local leaf (Fichman et al., 2019; Devireddy et al., 2020).

Systemic cell-to-cell ROS signals were previously found to be dependent on several different calcium-permeable channels including MSL3 (Supplemental Data Set 1; Fichman et al., 2021). We therefore used the method described above (Figure 2A) to test whether systemic cell-to-cell cytosolic calcium changes are dependent on MSL3. As shown in Figure 2B, in response to a local HL treatment, *msl3-1* and *msl3-2* mutants did not display local or systemic changes in cytosolic calcium levels. Furthermore, in contrast to WT, the *msl3-1* mutant did not display local or systemic changes in cytosolic calcium levels in response to a local treatment of 1-mM H_2O_2 (Supplemental Figure S1). These finding suggest that MSL3 could function downstream of HPCA1.

Systemic cell-to-cell calcium and ROS signals were previously proposed to be linked with another type of cell-to-cell signaling, termed the "electric wave", which is a rapid depolarization of the plasma membrane, also dependent on the function of GLRs (Mousavi et al., 2013; Nguyen et al., 2018; Farmer et al., 2020; Fichman and Mittler, 2021a). To determine whether HPCA1 is also required for systemic cell-to-cell membrane depolarization signals, we subjected a single leaf of WT, *hpca1-1*, and *hpca1-2* plants to the same HL stress treatment described above and used $DiBAC_4(3)$ as a probe in our live imaging platform (Fichman and Mittler, 2021a) to measure these changes in local and systemic

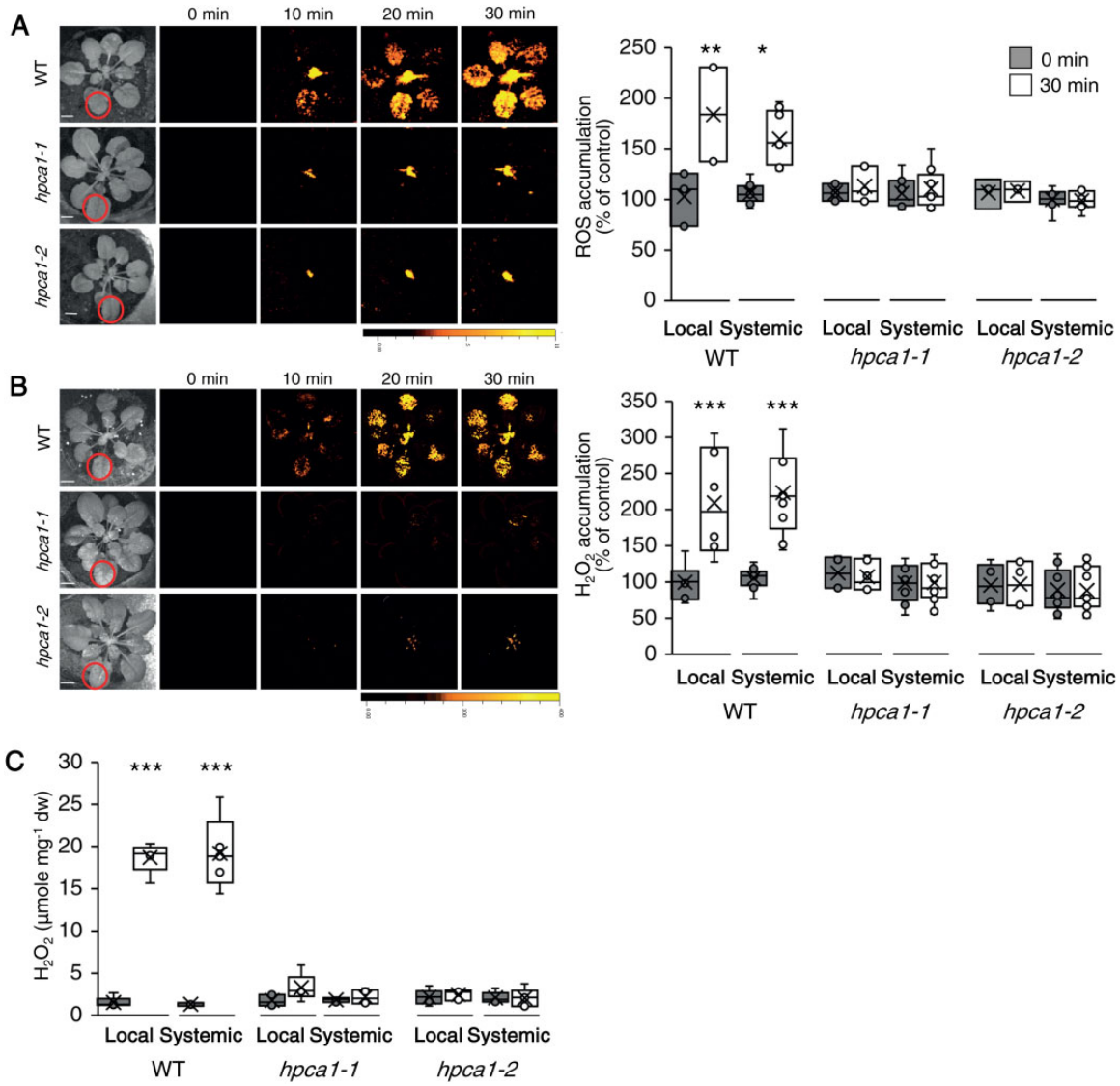

Figure 1 HPCA1 is required for systemic cell-to-cell ROS signaling in response to light stress. A, Arabidopsis plants were subjected to a HL stress treatment applied to a single leaf (Local; indicated with a circle), and ROS accumulation was imaged, using H_2DCFDA, in whole plants (local and systemic tissues). Representative time-lapse images of whole-plant ROS accumulation in WT, *hpca1-1* and *hpca1-2* plants are shown alongside bar graphs of combined data from all plants used for the analysis at the 0- and 30-min time points (local and systemic). B, Same as in (A), but for whole-plant H_2O_2 accumulation that was imaged using PO1. C, Arabidopsis plants were subjected to a HL stress treatment applied to a single leaf (Local) and the levels of H_2O_2 were measured in extracts from local and systemic leaves using Amplex-Red. All experiments were repeated at least three times with 10 plants of each genotype per experiment. Data are presented as box plot graphs; *X* is mean ± SE, $N = 30$, $^*P < 0.05$, $^{**}P < 0.01$, $^{***}P < 0.001$, Student *t* test. Scale bar, 1 cm. See Movie 1 for live imaging.

leaves over a period of 30 min. Interestingly, while the systemic cell-to-cell calcium and ROS signals were suppressed in the *hpca1* mutants (Figures 1 and 2; Movie 1), the rapid local and systemic membrane depolarization signal was not (Figure 3; Movie 1). In contrast to the *hpca1* mutants, and in agreement with our previous characterization of the *glr3.3 glr3.6* double mutant (Fichman and Mittler, 2021a), cell-to-cell membrane depolarization signals were suppressed in the *glr3.3 glr3.6* double mutant in response to a local application of HL stress (Figure 3).

The findings presented in Figures 1–3 suggest that HPCA1 is required for local accumulation of H_2O_2 during light stress, as well as for the activation of the calcium and ROS (but not electric) waves in response to a local treatment of HL stress.

HPCA1 is required for local and systemic expression of different acclimation-related transcripts as well as for local and systemic plant acclimation to HL stress

Suppression of systemic cell-to-cell ROS and/or calcium signals (Figures 1 and 2) could prevent plants from acclimating to stress. To test whether HPCA1 mutants are deficient in plant acclimation, we measured the local and systemic

expression of several transcripts associated with plant acclimation to excess light stress 30 min following the application of HL (1,700 µmol photons $s^{-1}m^{-2}$) stress for 2 min to a local leaf of WT and *hpca1-1* plants. As shown in Figure 4A, the expression of *MYELOBLASTOSIS DOMAIN PROTEIN 30 (MYB30)*, *ZINC FINGER OF A. THALIANA 10* and *12* (*ZAT10* and *ZAT12*), *ASCORBATE PEROXIDASE 2* (*APX2*), and *ZINC FINGER HOMEODOMAIN* 5 (*ZHD5*), was upregulated in local and systemic leaves of WT plants in response to the local HL stress treatment. In contrast, except for *APX2*, which was upregulated in local leaves of *hpca1-1* plants, the expression of all transcripts was suppressed in local and systemic leaves of *hpca1-1* plants in response the local HL stress treatment (Figure 4A).

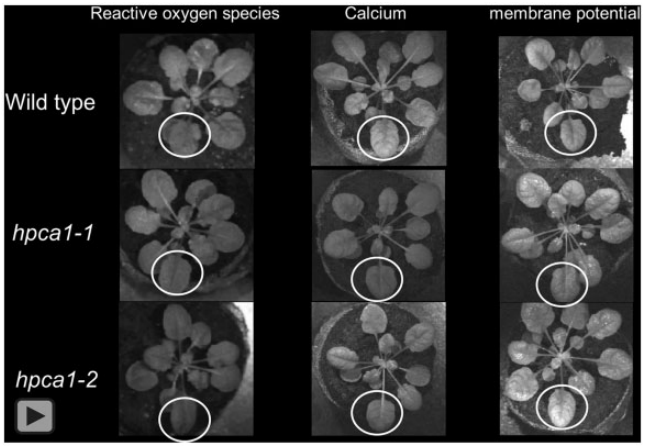

Movie 1 Live whole-plant imaging of changes in cell-to-cell ROS, calcium, and membrane potential signals in response to the application of HL stress to a single leaf (indicated by a white circle) of WT and two independent mutants of HPCA1 (*hpca1-1*, *hpca1-2*).

The lack of systemic ROS and calcium cell-to-cell signals (Figures 1 and 2), as well as systemic expression of *MYB30*, *ZAT10*, *ZAT12*, *APX2*, and *ZHD5* (Figure 4A), could suggest that HPCA1 is required for systemic acclimation of plants to HL stress. To test this possibility, we measured the acclimation (i.e. reduced tissue damage following exposure to light stress) of mature WT and *hpca1-1* plants to a prolonged HL stress treatment following a short pretreatment with HL stress and an incubation period. As shown in Figure 4B, pretreatment of WT plants with 10 min of HL stress, followed by an incubation of 50 min under controlled growth conditions, protected local and systemic leaves of plants from a subsequent exposure to 45 min of HL stress (i.e. prevented leaf injury as measured by electrolyte leakage, compared to

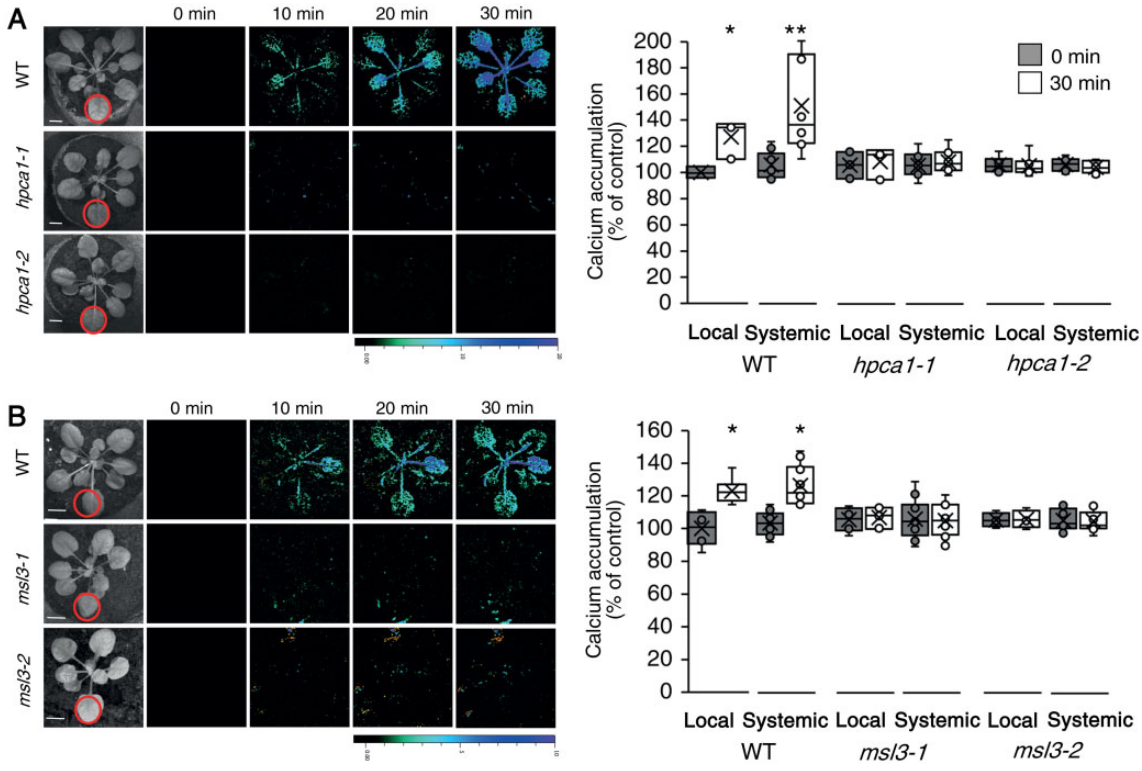

Figure 2 HPCA1 and MSL3 are required for systemic cell-to-cell calcium signaling in response to light stress. A, Arabidopsis plants were subjected to a HL stress treatment applied to a single leaf (Local; indicated with a circle), and cytosolic calcium accumulation was imaged using Fluo-4-AM in whole plants (local and systemic tissues). Representative time-lapse images of whole-plant cytosolic calcium accumulation in WT, *hpca1-1* and *hpca1-2* plants are shown alongside bar graphs of combined data from all plants used for the analysis at the 0- and 30-min time points (local and systemic). B, Same as in (A), but for WT, *msl3-1* and *msl3-2* plants. Compared to WT, the *msl3-1* mutant is also deficient in cell-to-cell calcium signaling in response to a local application of H_2O_2 (Supplementary Figure S1). All experiments were repeated at least three times with 10 plants of each genotype per experiment. Data are presented as box plot graphs; *X* is mean ± SE, $N = 30$, $^*P < 0.05$, $^{**}P < 0.01$, Student *t* test. Scale bar, 1 cm. See Movie 1 for live imaging.

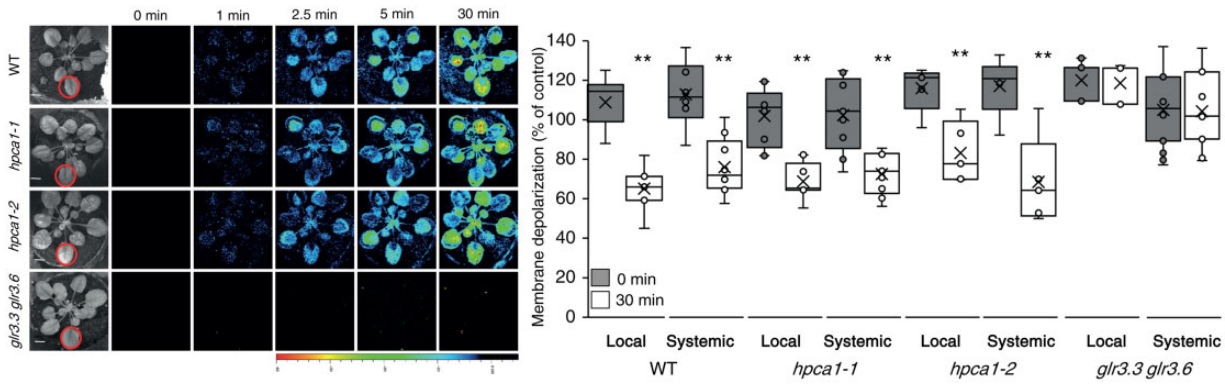

Figure 3 HPCA1 is not required for systemic cell-to-cell changes in membrane potential in response to light stress. Arabidopsis plants were subjected to a HL) stress treatment applied to a single leaf (Local; indicated with a circle), and changes in membrane potential were imaged using $DiBAC_4(3)$ in whole plants (local and systemic tissues). Representative time-lapse images of whole-plant changes in membrane potential in WT, *hpca1-1* and *hpca1-2* plants are shown alongside bar graphs of combined data from all plants used for the analysis at the 0- and 30-min time points (local and systemic). The double mutant *glr3.3 glr3.6*, that lacks a cell-to-cell membrane potential signal in response to HL stress (Fichman and Mittler 2021a), was used as a negative control. All experiments were repeated at least three times with 10 plants of each genotype per experiment. Data are presented as box plot graphs; *X* is mean ± SE, *N* = 30, $^{**}P < 0.01$, Student *t*-test. Scale bar, 1 cm. See Movie 1 for live imaging.

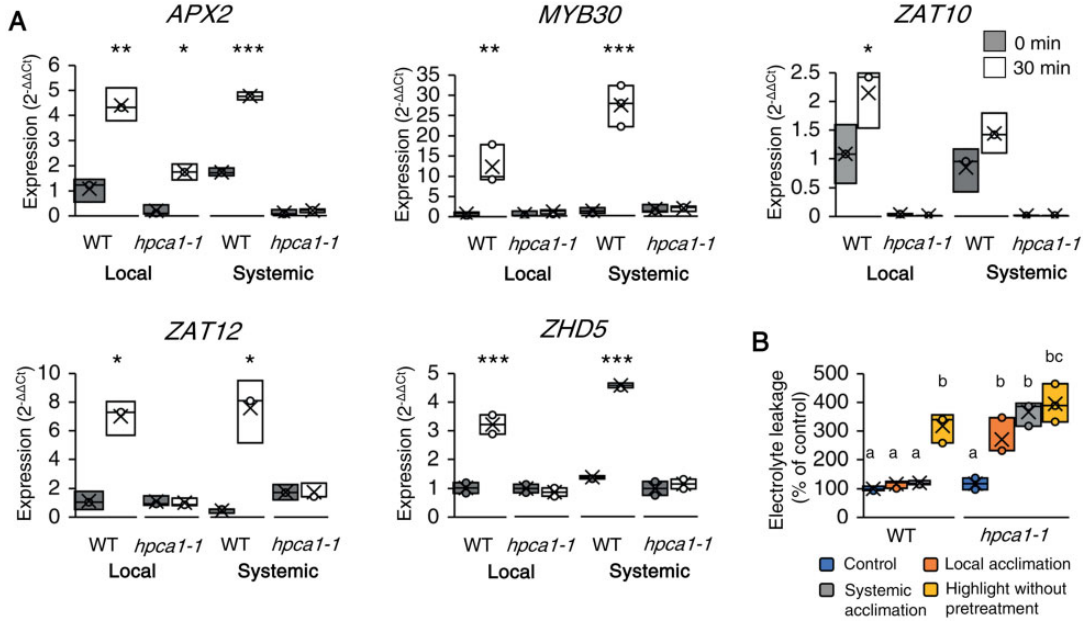

Figure 4 HPCA1 is required for local and systemic expression of stress-acclimation transcripts, as well as acclimation of plants to light stress. A, Real-time quantitative PCR analysis of *APX2*, *MYB30*, *ZAT10*, *ZAT12*, and *ZHD5* expression in local and systemic leaves of WT and *hpca1-1* plants subjected to a local HL treatment. Transcripts tested were previously found to respond to HL stress in WT plants. Results are presented as relative quantity (RQ) compared to control WT from local leaf. B, Averaged measurements of leaf injury (increase in ion leakage) of WT and *hpca1-1* plants. Measurements are shown for unstressed plants (control), local leaves subjected to a pretreatment of HL stress before a long HL stress period (local acclimation), systemic leaves of plants subjected to a local HL stress pretreatment before a long period of local HL stress was applied to a systemic leaf (systemic acclimation), and systemic leaves of plants subjected to a long HL stress period without pretreatment (HL without pretreatment). Results are presented as percent of control (leaves not exposed to HL stress). All experiments were repeated at least three times with 10 plants of each genotype per experiment. Data is presented in (A) as box plot graphs; *X* is mean ± SE, *N* = 30, $^{*}P < 0.05$, $^{**}P < 0.01$, $^{***}P < 0.001$, Student *t*-test. Data are presented in (B) as box plot graphs where *X* is mean ± SE, *N* = 30, one-way ANOVA followed by a Tukey test; lowercase letters donate significance ($P < 0.05$).

plants that were subjected to the 45-min HL treatment without a 10-min pretreatment with excess white or red light). In contrast, pretreatment of *hpca1-1* plants with a short HL stress failed to induce local or systemic leaf acclimation to a subsequent prolonged HL stress that resulted in a significant increase in electrolyte leakage from cells (Figure 4B).

The findings presented in Figure 4 suggest that although the HL stress is sensed at the local leaves of the *hpca1* mutants (evident by increased expression of *APX2*), these

mutants are deficient in many other aspects of local and systemic plant responses and acclimation to HL stress.

HPCA1 is required for the propagation of the HL-induced systemic ROS signal

Systemic cell-to-cell ROS signaling is driven by two different pathways, one that controls its initiation at the local tissue, and one that controls its propagation-, amplification-, and acclimation-promoting functions, in local and systemic tissues (Fichman et al., 2021; Mittler et al., 2022). In addition to these pathways, there are other systemic signaling pathways such as the calcium, membrane potential (electric), and stress-specific signals (Suzuki et al., 2013; Fichman et al., 2021; Fichman and Mittler, 2020a, 2021a; Mittler et al., 2022). The relationship between some of these systemic signals can be distinguished in plants by grafting experiments between WT plants and different mutants (Suzuki et al., 2013; Fichman et al., 2021). Using such grafting experiments, we found that HPCA1 is required for the propagation but not initiation of the HL-induced systemic ROS signal (Figure 5). Thus, while the *hpca1-1* mutant was deficient in ROS wave propagation through the scion (systemic tissue), following the activation of the ROS wave at the WT stock (that includes the local tissue), it could transmit other systemic signals that are not the ROS wave through the (local) stock tissue to a WT scion triggering in it the ROS wave (Figure 5, A–C). In contrast, the *rbohD* mutant was deficient in both systemic signal initiation and propagation (Figure 5D; Supplemental Figure S2; Fichman et al., 2021), while the *rbohF* mutant was similar to *hpca1-1* mutant and was only deficient in systemic ROS wave propagation (Figure 5E; Supplemental Figure S2).

HPCA1 is therefore required for the propagation of the systemic cell-to-cell ROS signal (Figure 5, A–C), as well as for its transcript accumulation- and acclimation-driven functions in systemic tissues (Figure 4). HPCA1 is however not required for some of the other systemic signals that can propagate through a stock that lacks HPCA1 (*hpca1*) into a WT scion and trigger in it the ROS wave. Because HPCA1 is not required for the membrane potential signal to propagate in response to a local HL stress treatment (Figure 3), but RBOHD is (Suzuki et al., 2013; Fichman and Mittler, 2021a), an electric wave produced by the local HL stress in the *hpca1* stock could be one of the other systemic signals that propagates through this stock into the WT scion triggering a ROS wave in the scion.

HPCA1 is required for systemic cell-to-cell ROS signaling in response to a local bacterial infection or salt stress, but not wounding

The findings that HPCA1 is required for the propagation of the ROS wave (Figure 5, A–C), which plays a key role in plant responses to many different abiotic stresses (Zhu, 2016; Fichman et al., 2019, 2021; Zandalinas et al., 2020a, 2020b; Fichman and Mittler, 2020b; Mittler et al., 2022), could suggest that HPCA1 is involved in plant responses to a broad range of stresses. To test the involvement of HPCA1 in local and systemic ROS responses to other stresses, we treated a local leaf of WT or *hpca1-1* plants with a bacterial pathogen (*Pseudomonas syringae* DC 3000; 10^6 CFU mL^{-1}; Fichman et al., 2019), salt stress (100-mM NaCl), or wounding (simultaneously piercing with 20 dress pins; Fichman et al., 2019), and measured local and systemic accumulation of ROS (untreated or mock buffer treatment in the absence of the pathogen or salt were used as controls). As shown in Figure 6, while all treatments caused the accumulation of ROS in local and systemic leaves of WT plants, *hpca1-1* plants did not respond to the bacterial pathogen or salt stress treatments (Figure 6, A and B). In response to a local treatment of wounding, *hpca1-1* mutants did however display a local and systemic cell-to-cell ROS signaling response that was indistinguishable from that of WT (Figure 6C). These findings suggest that cell-to-cell ROS signals could be mediated in plants by more than one type of ROS receptor. Systemic cell-to-cell ROS signaling pathways, triggered by HL stress, bacterial infection, or salinity treatments (Figures 1, 6, A and B) and mediated by HPCA1, could therefore be distinguished from those activated by wounding (Figure 6C) and potentially mediated by a yet unknown ROS receptor(s). In a previous study, treatment of *hpca1* seedlings with 100-mM NaCl triggered changes in calcium levels (Wu et al., 2020). In agreement with these studies, we also found that salt stress (100-mM NaCl) triggers a calcium wave in the *hpca1-1* mutant (Supplemental Figure S3) but not a ROS wave (Figure 6B). Salt stress (100-mM NaCl) was also found to trigger a calcium wave in *msl3-1* mutant (Supplemental Figure S3). Taken together, these findings suggest that the calcium wave could be mediated via different molecular mechanisms during HL and salt stresses [i.e. MSL3 during HL stress, as opposed to TWO-PORE CHANNEL 1 (TPC1) during salt stress; Figures 2 and 6 (Evans et al., 2016)]. Further studies are required to address the coupling of the ROS and calcium waves during salt, HL, and other biotic and abiotic stresses.

HPCA1-dependent cell-to-cell ROS signaling requires the central calcium signaling regulators CBL4, CIPK26, and OST1

The increase in calcium levels resulting from HPCA1 activation during local and systemic responses to HL stress (Figure 2) could cause the activation of calcium-dependent protein kinase cascades and trigger ROS production by RBOHs (Luan and Wang, 2021; Mittler et al., 2022). Our mutant screen (Supplemental Data Set 1) identified three proteins potentially involved in such cascades (CBL4, CIPK26, and OST1). As shown in Figure 7A, similar to the *hpca1-1* mutant (Figure 1), *cbl4-1*, *cipk26-2*, and *ost1-2* mutants were deficient in mediating the systemic cell-to-cell ROS signal in response to a 2 min local treatment of HL stress. In addition, and also similar to the *hpca1-1* mutant (Figure 4B), *cbl4-1*, *cipk26-2*, and *ost1-2* mutants were unable to acclimate to

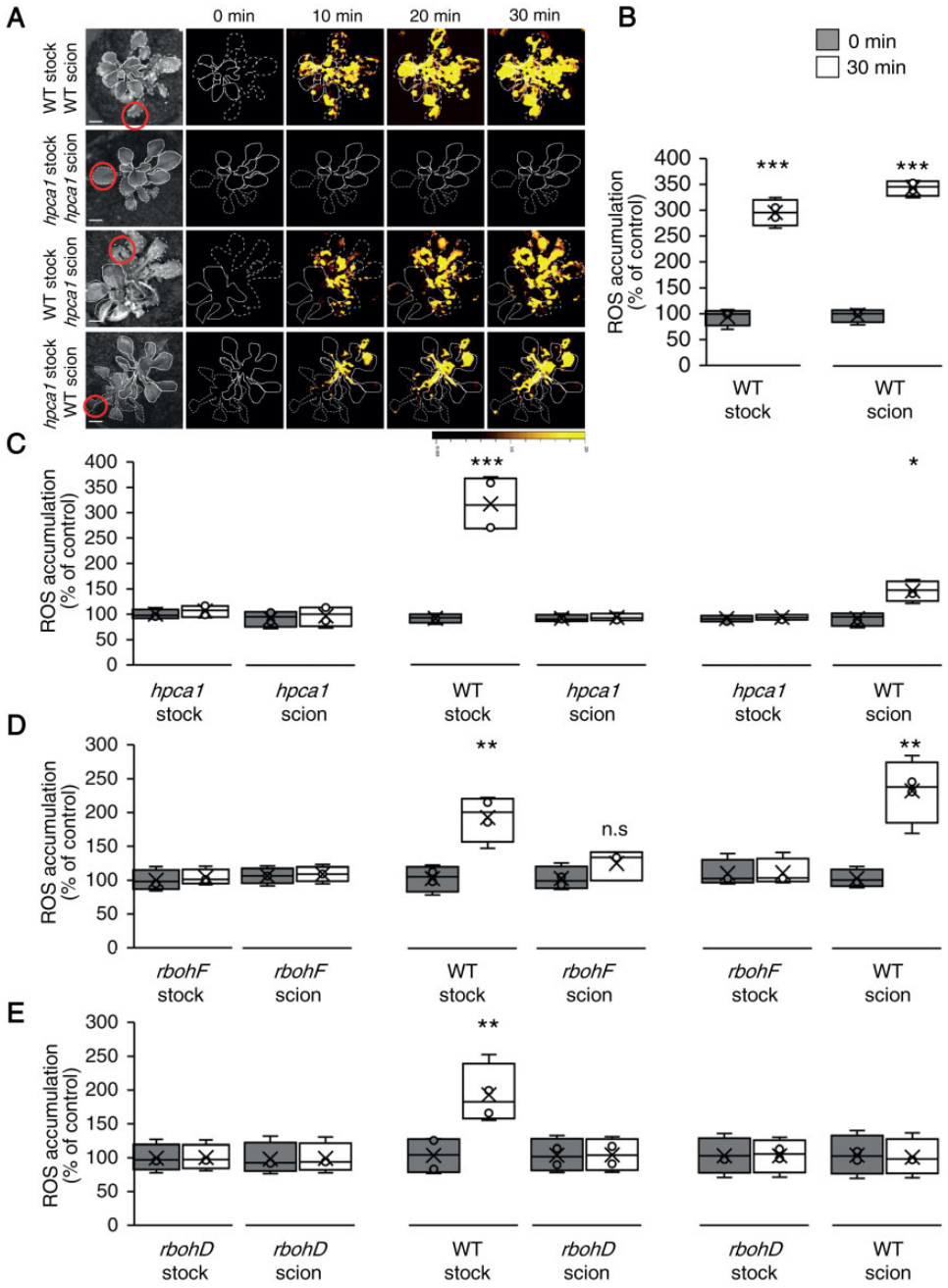

Figure 5 HPCA1 is required for systemic cell-to-cell ROS signal propagation, but not initiation, in response to light stress. A, Representative time-lapse images of ROS accumulation in stock and scion parts of grafted plants, generated using WT and *hpca1-1* plants, in response to HL stress applied to a single leaf (indicated with a circle) belonging to the stock part. Scions are indicated by solid white lines, and stocks are indicated by dashed white lines. B, Bar graphs showing the combined data from the stock and scion of grafted WT plants subjected to HL stress on a single leaf of the stock scion. C, Same as (B), but for different grafting combinations between WT and *hpca1-1* plants. D, Same as (B), but for different grafting combinations between WT and *rbohF* plants. E, Same as (B), but for different grafting combinations between WT and *rbohD* plants. Representative time-lapse images of ROS accumulation in stock and scion parts of grafted WT and *rbohD*, or *rbohF*, plants are shown in Supplementary Figure S2. All experiments were repeated at least three times with 10 plants of each genotype per experiment. ROS accumulation was imaged using H_2DCFDA. Data are presented as box plot graphs; *X* is mean ± SE, $N = 30$, $^*P < 0.05$, $^{**}P < 0.01$, $^{***}P < 0.001$, Student's *t* test. Scale bar, 1 cm.

HL stress following a pretreatment with a short period of HL stress (Figure 7B).

To test whether CBL4, CIPK26, and OST1 are required for the initiation or propagation of the systemic cell-to-cell ROS signal, we conducted grafting experiments between these mutants and WT plants (Figure 8; similar to the analysis described in Figure 5). These studies revealed that like HPCA1 (Figure 5), CBL4, CIPK26, and OST1 are all required for the

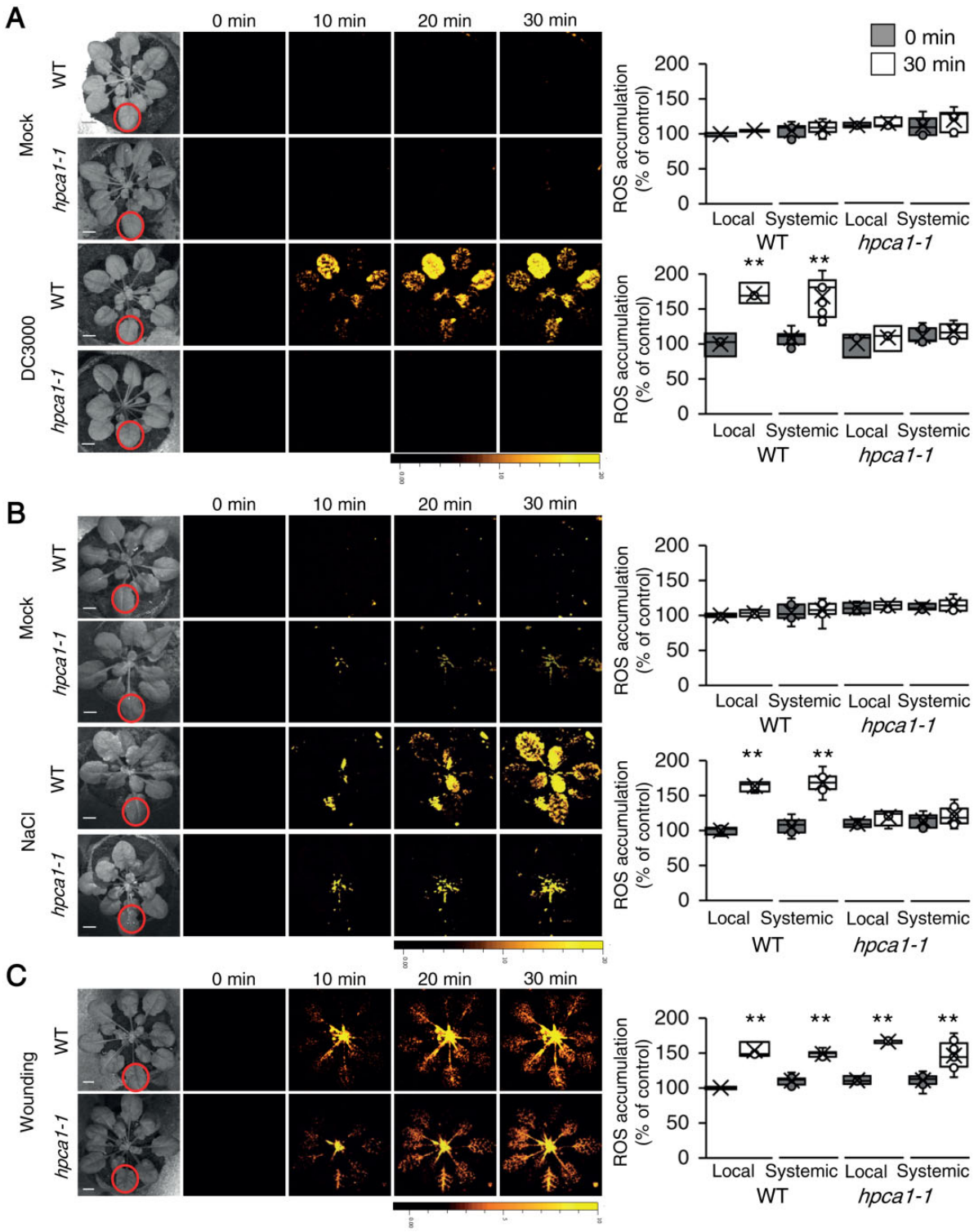

Figure 6 HPCA1 is required for systemic cell-to-cell ROS responses to bacterial infection and salt stress, but not wounding. A, Representative time-lapse images of whole-plant ROS accumulation in WT and *hpca1-1* plants subjected to mock or bacterial (*Pseudomonas syringae* DC3000) infection on a single local leaf are shown alongside bar graphs of combined data from all plants used for the analysis at the 0- and 30-min time points (local and systemic). B, Same as in (A), but for mock and salt stress (100-mM NaCl) applied to a single local leaf. C, Same as in (A), but for wounding applied to a single local leaf (control plants were untreated). Although the *hpca1-1* mutant is deficient in cell-to-cell ROS signaling in response to salinity stress (B), it displays cell-to-cell calcium signaling in response to this stress (Supplemental Figure S3). All experiments were repeated at least three times with 10 plants of each genotype per experiment. ROS accumulation was imaged using H_2DCFDA. Data are presented as box plot graphs; X is mean ± SE, $N = 30$, $^{**}P < 0.01$, Student *t* test. Scale bar, 1 cm.

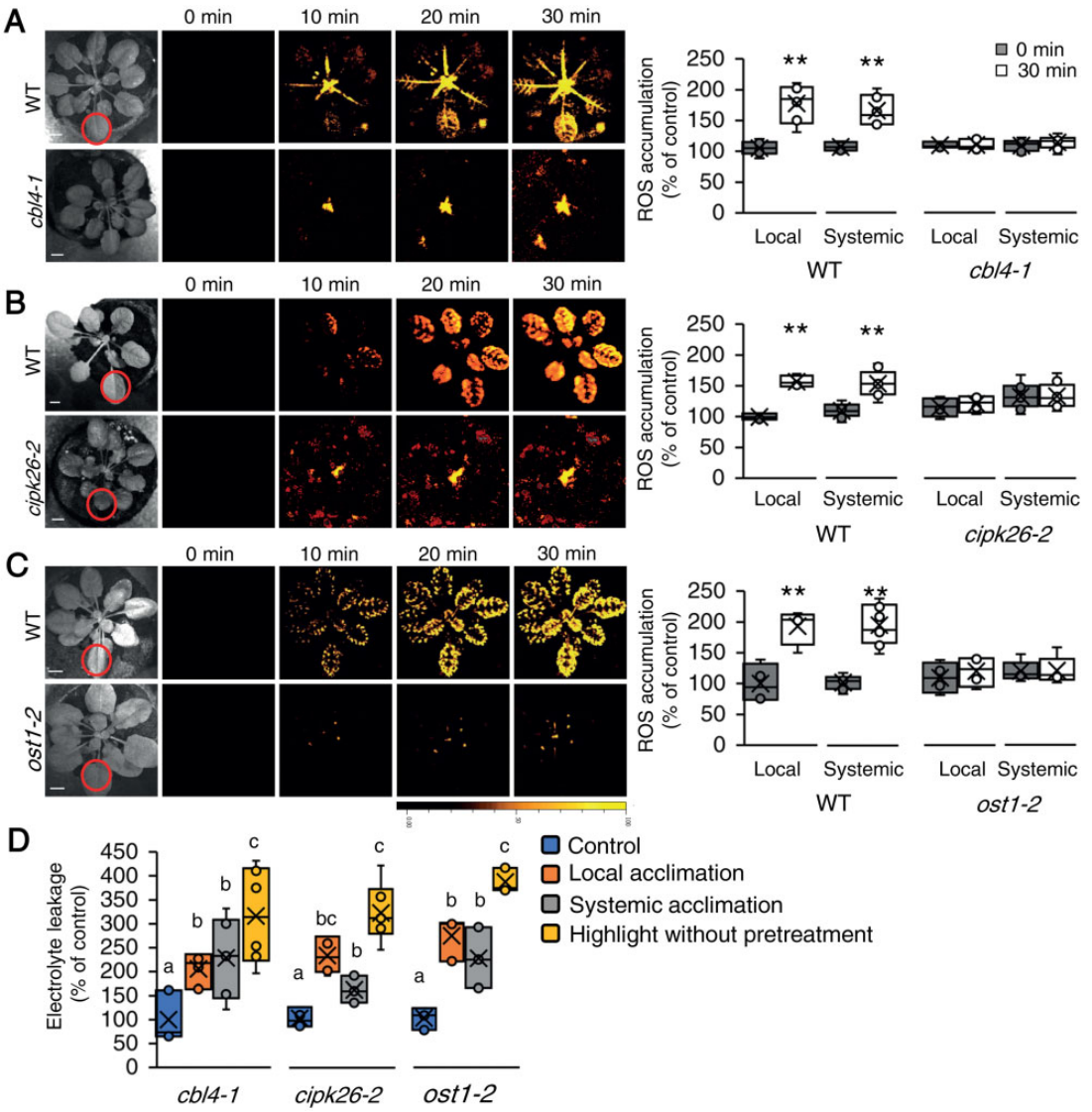

Figure 7 CBL4, CIPK26, and OST1 are required for systemic cell-to-cell ROS signaling and acclimation to light stress. A, Representative time-lapse images of whole-plant ROS accumulation in WT and *cbl4-1* plants subjected to a local HL stress treatment (applied to a single local leaf; indicated with a circle) are shown alongside bar graphs of combined data from all plants used for the analysis at the 0- and 30-min time points (local and systemic). B, Same as (A), but for WT and *cipk26-2* plants. C, Same as (A), but for WT and *ost1-2* plants. D, Averaged measurements of leaf injury (increase in ion leakage) in WT, *cbl4*, *cipk26*, and *ost1* plants. Measurements are shown for unstressed plants (control), local leaves subjected to a pretreatment of HL stress before a long HL stress period (local acclimation), systemic leaves of plants subjected to a local HL stress pretreatment before a long period of local HL stress was applied to a systemic leaf (systemic acclimation), and systemic leaves of plants subjected to a long HL stress period without pretreatment (HL without pretreatment). All experiments were repeated at least three times with 10 plants of each genotype per experiment. ROS accumulation was imaged using H_2DCFDA. Data are presented in (A) to (C) as box plot graphs; *X* is mean ± SE, *N* = 30, $^{**}P < 0.01$, Student *t* test. Data are presented in (D) as box plot graphs; X is mean ± SE, *N* = 30, one-way ANOVA followed by a Tukey test; lowercase letters donate significance ($P < 0.05$). Scale bar, 1 cm.

propagation of the systemic cell-to-cell ROS signal. Thus, while the *cbl4-1*, *cipk26-2*, and *ost1-2* mutants were deficient in ROS wave propagation through the scion (systemic tissue), following the activation of the ROS wave at the WT stock (that includes the local tissue), they could transmit other HL-induced systemic signals that are not the ROS wave through the (local) stock tissue to a WT scion and trigger in it the ROS wave (Figure 8). The findings that key components of a calcium-dependent signaling cascade (i.e. CBL4, CIPK26, and OST1) are required for the propagation of the cell-to-cell ROS signal reveal that enhanced levels of calcium alone (Figure 2) are not sufficient to trigger the ROS wave by directly interacting with the calcium-binding domains of RBOHD (Ogasawara et al., 2008). Rather, an amplification cascade of the signal is needed. The results presented in Figures 3, 5, 7, and 8 also suggest that HPCA1, CBL4, CIPK26, and OST1 are not required for the propagation of other HL-induced systemic signals such as the

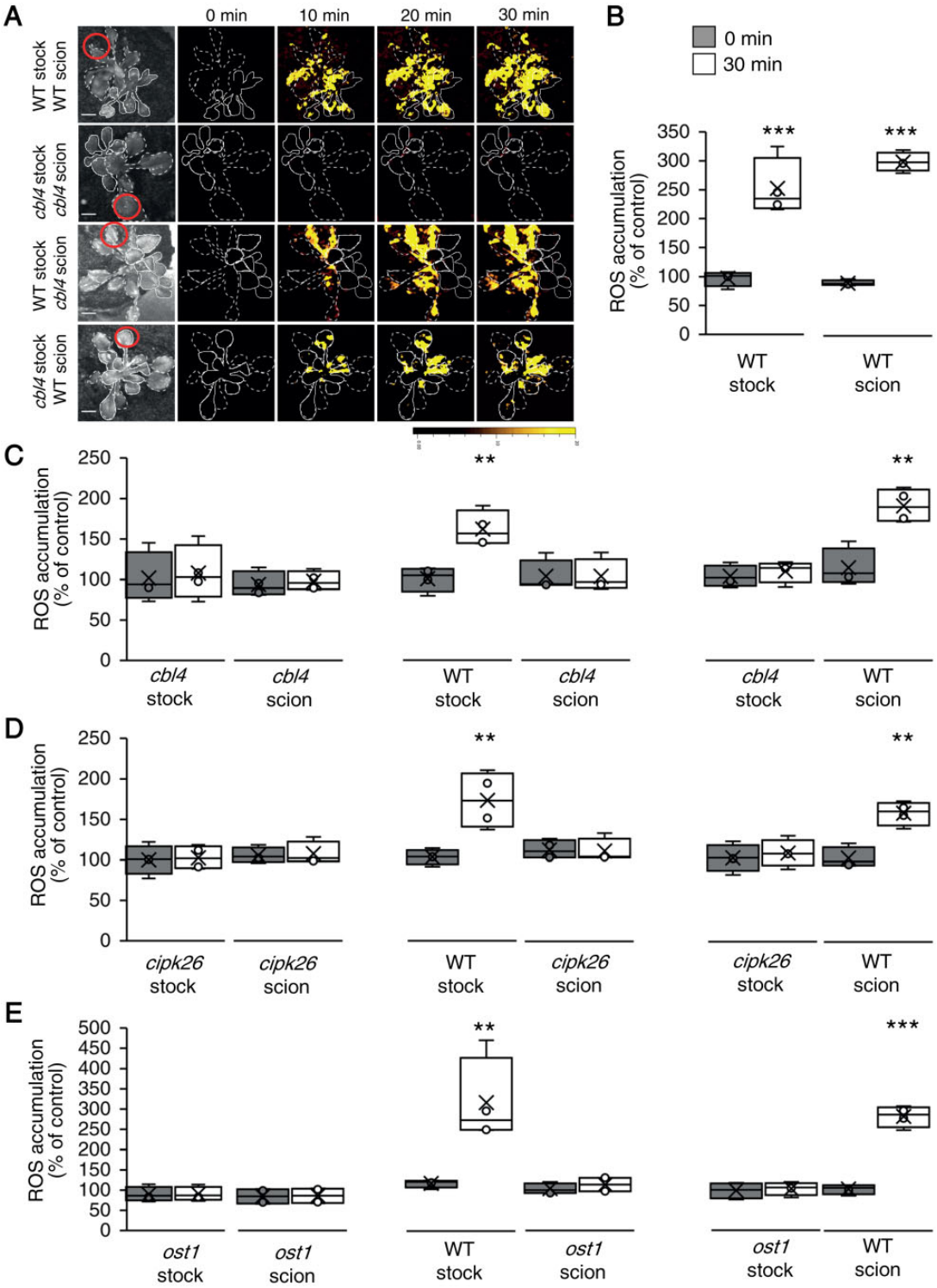

Figure 8 CBL4, CIPK26, and OST1 are required for systemic ROS signal propagation, but not initiation, in response to light stress. A, Representative time-lapse images of ROS accumulation in stock and scion parts of grafted plants, generated using WT and *cbl4-1* plants, in response to a local HL stress treatment applied to a single leaf (indicated with a circle) belonging to the stock part. Scions are indicated by solid white lines, and stocks are indicated by dashed white lines. B, Bar graphs showing the combined data from the stock and scion of grafted WT plants subjected to HL stress on a single leaf of the stock scion. C, Same as (B), but for different grafting combinations between WT and *cbl4-1* plants. D, Same as (B), but for different grafting combinations between WT and *cipk26-2* plants. E, Same as (B), but for different grafting combinations between WT and *ost1-2* plants. All experiments were repeated at least three times with 10 plants of each genotype per experiment. ROS accumulation was imaged using H_2DCFDA. Data are presented as box plot graphs; *X* is mean ± SE, $N = 30$, $^{**}P < 0.01$, $^{***}P < 0.001$, Student *t* test. Scale bar, 1 cm.

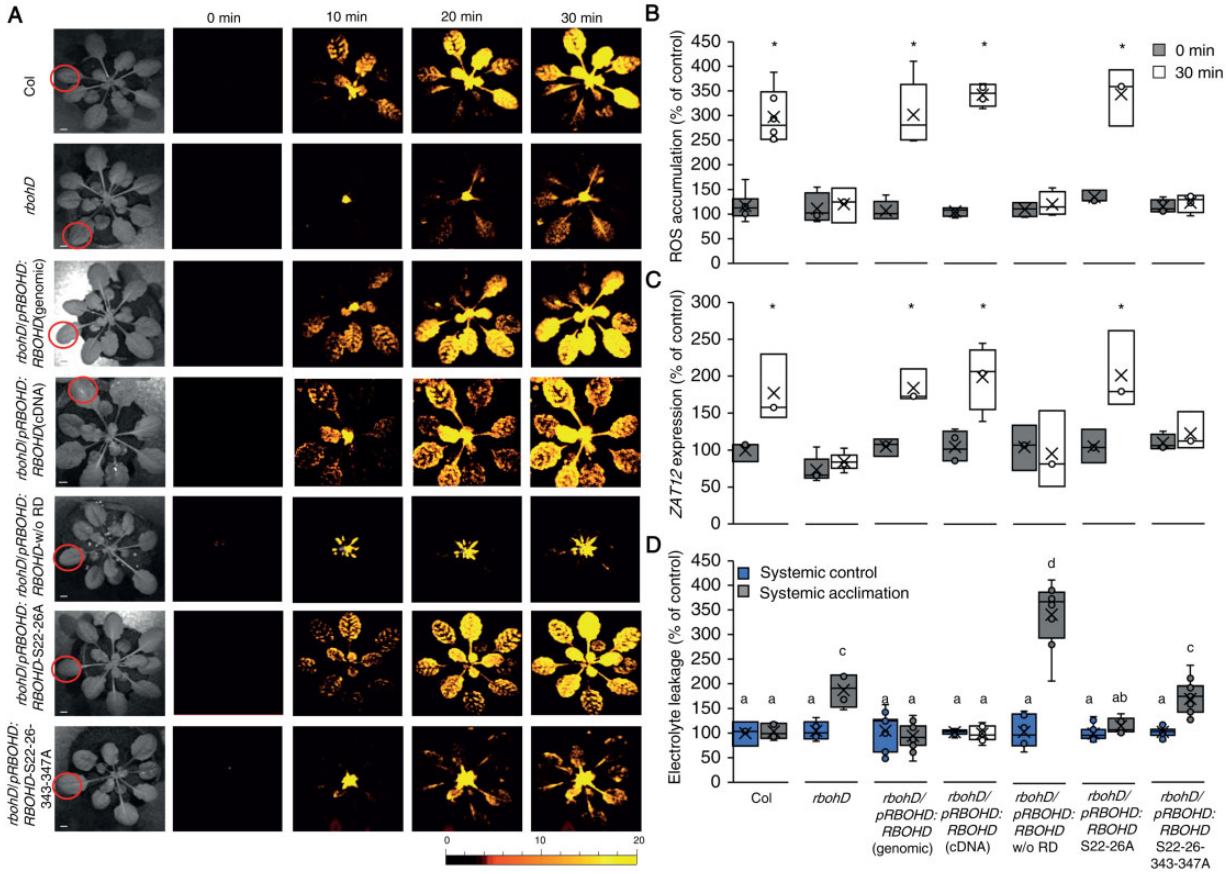

Figure 9 Mutating specific amino acids in RBOHD suppresses systemic ROS accumulation in response to HL stress. A, Representative time-lapse images of whole-plant ROS accumulation in WT, *rbohD*, *rbohD* complemented with the WT *RBOHD* gene [*rbohD pRBOHD:RBOHD* (genomic)], *rbohD* complemented with the *RBOHD* cDNA expressed under the control of the *RBOHD* promoter [*rbohD pRBOHD:RBOHD* (cDNA)], *rbohD* complemented with the *RBOHD* cDNA without the N-terminal RD (1–347) expressed under the control of the *RBOHD* promoter [*rbohD pRBOHD: RBOHD* w/o RD], *rbohD* complemented with the *RBOHD* gene with S22A and S26A mutations [*rbohD pRBOHD:RBOHD* S22–26A], or *rbohD* complemented with the *RBOHD* gene with S22A, S26A, S343A, and S347A mutations [*rbohD pRBOHD:RBOHD* S22–26–343–347A], following treatment of a single local leaf with HL stress (indicated with a circle). B, Bar graphs of combined data from all plants used for the analysis shown in (A) at the 0- and 30-min time points (systemic). C, Bar graphs of combined *ZAT12* promoter activity (luciferase imaging) in systemic leaves of *rbohD ZAT12:luciferase* double homozygous plants transformed with all vectors shown in (A), measured at 0- and 30-min time following application of HL stress to a single local leaf. D, Averaged measurements of leaf injury (increase in ion leakage) in systemic tissues of all lines shown in (A). Measurements are shown for unstressed systemic leaves (systemic control) and systemic leaves of plants subjected to a local HL stress pretreatment before a long period of local HL stress was applied to a systemic leaf (systemic acclimation). All experiments were repeated at least three times with 10 plants of each genotype per experiment. Two independent transgenic lines for each construct were averaged. ROS accumulation was imaged using H_2DCFDA. Data presented in (B) and (C) are mean ± SE, $N = 30$, $^*P < 0.05$, Student *t* test. Data presented in (D) are mean ± SE, $N = 30$, one-way ANOVA followed by a Tukey test; lowercase letters donate significance ($P < 0.05$). Scale bar, 1 cm.

electric wave that are initiated in the local tissue (stock; Figure 3).

The same amino acid residue required for RBOHD activation by OST1 is also required for RBOHD activation during systemic cell-to-cell ROS signaling

The sensing of high cytosolic calcium levels by CBL4 was shown to activate CIPK26, and CIPK26 was shown to phosphorylate and activate RBOHF (Drerup et al., 2013). CIPK26 was also shown to interact with OST1 (Mogami et al., 2015). OST1, in turn, is thought to phosphorylate RBOHD on serine 347 and activate it (Wang et al., 2020). OST1 was also shown to phosphorylate and activate RBOHF (Sirichandra et al., 2009). Because RBOHD plays such a canonical role in the initiation and propagation of the systemic cell-to-cell ROS signal (Figure 5; Supplemental Figure S2; Zandalinas et al., 2020a; Zandalinas et al., 2020b; Fichman et al., 2021), we tested whether deleting its N-terminal regulatory domain (RD; amino acids 1–347), or mutating serine 347 to alanine (the target of OST1 phosphorylation; Wang et al., 2020), will inhibit the systemic cell-to-cell ROS signal in response to HL stress. For this purpose, we expressed the WT *RBOHD* gene (*RBOHD* genomic; Figure 9), or the *RBOHD* cDNA (*RBOHD* cDNA; Figure 9), under the control of the *RBOHD* promoter in *rbohD* mutants. In addition, we expressed the *RBOHD* cDNA without the RD (*RBOHD* w/o RD; Figure 9), or the *RBOHD* gene with point mutations (serine to alanine) in

positions 22 and 26 (RbohD S22–26A; Figure 9), or 22, 26, 343, and 347 (*RBOHD* S22–26-343-347A; Figure 9) in the *rbohD* mutant (Nühse et al., 2007; Zandalinas et al., 2020b). Phosphorylation of RBOHD on S343/S347, as well as on S22/S26 was previously associated with the RBOHD- and ROS-dependent innate immune response of Arabidopsis (with S343/S347 playing a key role in this response; Nühse et al., 2007), and the WT *RBOHD* gene expressed under the control of the *RBOHD* promoter was shown to complement local and systemic ROS production in response to HL stress in the *rbohD* mutant (Zandalinas et al., 2020b). Once we confirmed that all transgenic complementation assays were homozygous and expressing a single copy of the transgene, we subjected a single leaf of WT, *rbohD*, *rbohD RBOHD* genomic, *rbohD RBOHD* cDNA, *rbohD RBOHD* w/o RD, *rbohD RBOHD* S22–26A, and *rbohD RBOHD* S22–26–343–347A to a 2 min of HL stress treatment (as described for Figure 1) and measured ROS accumulation in local and systemic leaves. As shown in Figure 9, A and B, complementation of the *rbohD* mutant with the WT *RBOHD*, WT *RBOHD* cDNA, or *RBOHD* S22–26A restored the systemic cell-to-cell ROS response. In contrast, complementation of the *rbohD* mutant with the *RBOHD* w/o RD, or the *RBOHD* S22–26–343–347A failed to restore the systemic ROS signal.

To study the expression of the key HL acclimation response gene *ZAT12* in *rbohD* mutants transformed with the different constructs, we conducted the same analysis described above; however, instead of the *rbohD* mutant we used the double homozygous line expressing the *ZAT12:luciferase* reporter in the *rbohD* background (developed as described in Miller et al., 2009; Zandalinas et al., 2020b) for the complementation study. As shown in Figure 9C, expression of the *ZAT12* gene (measured by luciferase activity; Miller et al., 2009; Zandalinas et al., 2020b) was significantly elevated only in *rbohD ZAT12:luciferase* lines complemented with the WT *RBOHD*, WT *RBOHD* cDNA, or *RBOHD* S22–26A (as well as in WT plants transformed with the *ZAT12:luciferase* reporter). In contrast, *ZAT12* expression was not complemented in *rbohD ZAT12:luciferase* lines by expression of the *RBOHD* w/o RD or the *RBOHD* S22–26–343–347A constructs. These findings agreed with the measurements of local and systemic ROS shown for the different complemented *rbohD* lines in parts A and B.

To study systemic acclimation to HL stress we also subjected the *rbohD* complemented lines (Figure 9, A and B) to the same HL SAA assay shown in Figures 4, B and 7, B. As shown in Figure 9D, complementation of the *rbohD* mutant with the WT *RBOHD*, WT *RBOHD* cDNA, or *RBOHD* S22–26A restored systemic HL acclimation to the *rbohD* mutant, while complementation of the *rbohD* mutant with the *RBOHD* w/o RD or the *RBOHD* S22–26–343–347A construct did not.

Taken together, the analyses shown in Figure 9 suggest that complementation of *rbohD* with the WT *RBOHD* gene, cDNA, or *RBOHD* gene with mutations in S22 and S26 (Nühse et al., 2007; Zandalinas et al., 2020b), restored HL-induced systemic cell-to-cell ROS signaling (Figure 9A), systemic *ZAT12* gene expression (Figure 9B), and systemic acclimation to HL stress (Figure 9C). By contrast, complementation of *rbohD* with the *RBOHD* cDNA that lacks the RD, or the *RBOHD* gene that contains point mutations in S22, S26, S343, and S347 (Nühse et al., 2007), did not restore the ROS wave, systemic *ZAT12* expression, or systemic acclimation to HL (Figure 9). These findings point to residues S343 and S347 (the target of OST1; Wang et al., 2020) as playing a key role in cell-to-cell ROS signaling.

Discussion

The ability of plants to mobilize a signal from a small group of cells subjected to stress to the entire plant, i.e., systemic signaling, plays a pivotal role in plant acclimation to, and/or defense against, many different abiotic and biotic stresses (Mittler et al., 2011, 2022; Zhu, 2016; Waszczak et al., 2018; Smirnoff and Arnaud, 2019; Farmer et al., 2020; Johns et al., 2021). Among the different signal transduction mechanisms that mediate systemic responses in plants is a rapid cell-to-cell signaling process that involves membrane depolarization, cytosolic calcium alterations, and ROS accumulation (Figures 1–3; Movie 1; Mittler et al., 2011, 2022; Farmer et al., 2020; Fichman and Mittler, 2020a; Shao et al., 2020; Johns et al., 2021). Previous studies identified RBOHD, RBOHF, and GLR3.3/GLR3.6 as key players in this cell-to-cell response (Miller et al., 2009; Mousavi et al., 2013; Toyota et al., 2018; Shao et al., 2020; Zandalinas et al., 2020b). While RBOHs were shown to mediate ROS production required for cell-to-cell signaling and plant acclimation (Miller et al., 2009; Fichman et al., 2019), GLRs were shown to mediate membrane depolarization and alterations in calcium levels (that could potentially drive ROS production; Mousavi et al., 2013; Evans et al., 2016; Toyota et al., 2018; Nguyen et al., 2018; Shao et al., 2020; Fichman and Mittler, 2021a). Prior studies have also suggested that the function of RBOHs and GLRs is interlinked (e.g. Fichman and Mittler, 2020a, 2021a). Nevertheless, how changes in ROS levels at the apoplast (produced by RBOHs) are translated into changes in cytosolic calcium during cell-to-cell ROS signaling remains unknown.

Here we show that HPCA1 plays a canonical role in systemic cell-to-cell signaling in plants, triggering cytosolic calcium accumulation upon sensing of apoplastic ROS/H_2O_2 (Figures 1 and 2, A; Movie 1). The altered calcium levels, potentially driven by MSL3 (Figure 2B; Supplemental Figure S1), could then activate a downstream pathway that requires CBL4, CIPK26, and OST1 and trigger further ROS production (Figures 7–9). HPCA1 may therefore represent a highly important and missing puzzle piece that links changes in apoplastic ROS levels driven by RBOH function with changes in cytosolic calcium levels driven by different calcium-permeable channels such as MSL3 (Figure 10). The finding that HPCA1 is required for systemic ROS and calcium cell-to-cell signaling (Figures 1 and 2, A), the expression of many acclimation transcripts in local and systemic tissues (Figure 4A), as well as plant acclimation (Figure 4B),

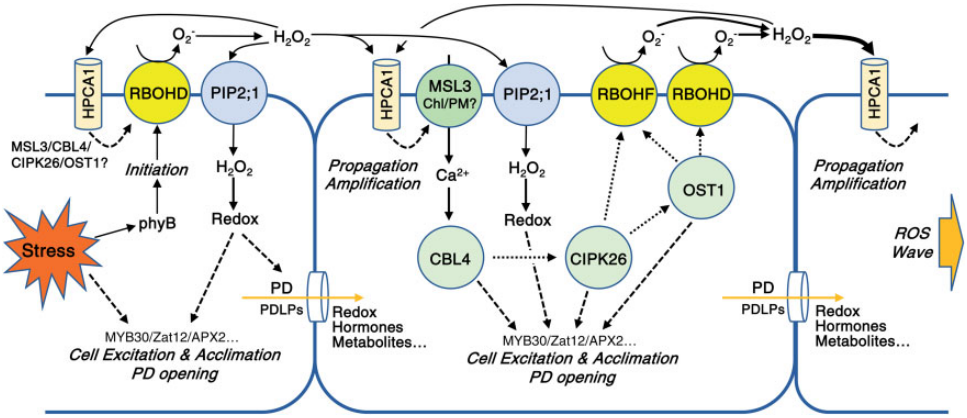

Figure 10 A model depicting the role of HPCA1 in the amplification and propagation of cell-to-cell ROS signaling in plants. HPCA1 is proposed to sense ROS at the apoplast and trigger an increase in cytosolic calcium levels via MSL3. The increase in calcium is proposed to activate a kinase cascade involving CBL4, CIPK26, and OST1 that activates RBOHD and RBOHF enhancing ROS production at the apoplast. The enhanced apoplastic ROS levels are sensed by the HPCA1 of the next cell in the cell-to-cell chain causing the enhanced apoplastic production of ROS by this cell, and a cell-to-cell ROS signaling process (the ROS wave) is formed. The enhanced apoplastic levels of ROS sensed by HPCA1 in each cell are also causing a positive amplification loop that further enhances ROS production in each cell of the cell-to-cell chain, including the initiating cell. ROS that accumulate in the apoplast (mainly H_2O_2) are shown to enter the cell via aquaporins and alter the redox state of different transcriptional regulators. The function of the pathway activated by HPCA1 is shown to be required for the enhanced transcript expression, acclimation, and resilience of plants to stress (please see text for more details). Dotted (for protein–protein interactions) and dashed (for regulatory effect) arrows are hypothetical.

provides strong support to this proposed role of HPCA1. Because some of the interactions between CBL4, CIPK26, OST1, and RBOHD/F were identified in vitro (e.g. Wang et al., 2020), further studies would be needed to dissect the calcium signaling cascades that function downstream of HPCA1. Additional studies are also required to identify the mode of HPCA1 activation during this process (Wu et al., 2020).

Interestingly, in our hands, HPCA1 appears not to be needed for the mediation of systemic membrane potential changes (Figure 3; Movie 1). In this respect it should also be noted that our grafting experiments (Figure 5) revealed that the mobilization of other HL-induced systemic signals, that are not the ROS wave, through a scion made from *hpca1-1* (without the accumulation of detectable ROS levels) could lead to the activation of the ROS cell-to-cell signal in the WT scion (Figure 5). Taken together, these findings suggest that a cell-to-cell membrane potential signal could mediate the HL-induced systemic signal in the *hpca1* mutant even in the absence of the ROS and/or calcium cell-to-cell signals (Figures 1–3, and 5; Movie 1). HPCA1 is however required in local and systemic plant tissues to enhance transcript expression and acquire a heightened state of acclimation; Figure 4). The notion that the electric wave could be playing a role in mediating systemic signaling to a local HL stress is also supported by the pace of the different systemic signals detected in our study (Figures 1–3; Movie 1). The systemic change in membrane potential (a type of electric wave) is the fastest, followed by a change in cell-to-cell cytosolic calcium levels, that are followed by changes in cell-to-cell ROS levels (Figures 1–3; Movie 1). These observations could suggest that an electric wave (that is GLR-dependent, at least for its initiation; Mousavi et al., 2013; Nguyen et al., 2018; Fichman and Mittler, 2021a) is the first to reach all cells.

The changes in membrane potential it brings with it may prime, alter, or activate different channels and other signaling mechanisms. These could then trigger a calcium wave that could be dependent on GLRs, MSLs, TPC1, and/or cyclic nucleotide-gated ion channels (CNGCs; Evans et al., 2016; Toyota et al., 2018; Shao et al., 2020; Fichman et al., 2021; Dickinson et al., 2022), that in turn activate ROS production via CBL4-, CIPK26- and/or OST1-mediated RBOH activation (Figures 7–10). Although calcium changes are imaged in our system before ROS changes (Figures 1–3; Movie 1), the new player in this pathway, introduced by this work, that is HPCA1, appears to be required for integrating the cell-to-cell calcium and ROS signals, providing a mechanistic understanding to how changes in apoplastic ROS levels are linked to changes in cytosolic calcium levels (Figure 10; Movie 1). The possible role of electric signals in activating cell-to-cell ROS signaling is also supported by a recent study showing that aboveground plant-to-plant transmission of electric signals (via two physically touching leaves) can trigger the cell-to-cell ROS signal in a receiving plant, and that this communication process is dependent on GLRs, RBOHs, and MSLs (Szechynska-Hebda et al., 2022). In addition, as shown in Figure 5E and Supplemental Figure S2, as well as reported previously (Fichman et al., 2021), a HL-induced systemic signal cannot propagate through a stock made from the *rbohD* mutant and trigger the ROS wave in a WT scion. In this respect it should be noted that RBOHD is required for the propagation of the electric wave in response to a local application of HL stress (Suzuki et al., 2013; Fichman and Mittler, 2021a). The electric wave that

propagates independently of HPCA1 (Figure 3) could therefore trigger the ROS and calcium waves that are dependent on each other, as well as on HPCA1 (Figures 1–3, 5, 7; Supplemental Figure S2; Movie 1), providing a possible hierarchy for systemic signaling in response to a local treatment of HL stress.

Interestingly, although HPCA1 was found to be required for systemic cell-to-cell ROS responses to local HL, salt, or pathogen treatments (Figures 1 and 6), it was not required for cell-to-cell ROS signaling in response to wounding (Figure 6). This finding could suggest that different receptors for apoplastic ROS are involved in mediating systemic cell-to-cell signaling in response to different stresses. Alternatively, the sensing of changes in apoplastic ROS levels may not play a key role in systemic cell-to-cell signaling in response to wounding. In this respect it should be noted that in addition to being sensed at the plasma membrane by HPCA1, ROS (H_2O_2) can also enter the cytosol from the apoplast through aquaporins (Rodrigues et al., 2017; Fichman et al., 2021; Figure 10). A recent study has shown for example that in the aquaporin mutant *plasma membrane intrinsic protein 2;1* (*pip2;1*), the cell-to-cell ROS signal triggered by HL stress is abolished (Fichman et al., 2021; Mittler et al., 2022). ROS could also move from cell-to-cell via plasmodesmata that open in an RBOHD-dependent manner during the progression of the cell-to-cell signal (Fichman et al., 2021). We previously showed that systemic cell-to-cell ROS responses are only suppressed in the *glr3.3glr3.6* double mutant in response to HL stress but are completely abolished in response to wounding (Fichman et al., 2021; Fichman and Mittler, 2021a). Systemic responses to wounding may therefore be more dependent on GLRs and other apoplastic and/or cytosolic ROS sensors, compared to systemic responses to HL stress (Mousavi et al., 2013; Toyota et al., 2018; Shao et al., 2020; Fichman and Mittler, 2021a; Mittler et al., 2022). In addition, they could be mediated through different cell layers that use different mechanisms for systemic cell-to-cell ROS signaling (i.e. mesophyll compared to vascular; Zandalinas et al., 2020b). Further studies are needed to address the relationships between different types of stress and apoplastic sensing of ROS via HPCA1, cytosolic sensing of ROS following their entry into the cell via aquaporins, and the transfer of ROS from cell-to-cell via plasmodesmata (Figure 10; Fichman et al., 2021).

In addition to its role in propagating the ROS wave (Figure 5), HPCA1 is also playing a role in ROS and calcium accumulation at the local tissue that is directly exposed to the HL stress (Figures 1 and 2). Moreover, HPCA1 is required for the expression of several stress–response transcripts at the local tissue (but not *APX2*) and for acclimation of the local tissue to HL stress (Figure 4). These findings suggest that HPCA1 plays a role in the sensing of the stress at the local tissue. We previously showed that the activation of RBOHD by HL stress at the local tissue requires Phytochrome B (phyB; Devireddy et al., 2020; Fichman et al., 2022; Figure 10). Light stress, that is sensed by chloroplasts could therefore trigger RBOHD via phyB at the local tissue, and the ROS produced by RBOHD could be sensed by HPCA1 leading to further activation of RBOHD in a positive feedback loop that is required for ROS accumulation, defense mechanism activation, and acclimation to HL stress at the local tissue (Figures 1, 4, and 10; Mittler et al., 2022).

An overall view of rapid cell-to-cell ROS and calcium signaling emerges from our study. In this view each cell in the cell-to-cell ROS signaling pathway senses the ROS generated by the cell preceding it via HPCA1, activates a calcium-dependent signal transduction pathway (involving CBL4, CIPK26, and OST1), and triggers ROS production by RBOHD and RBOHF (Figure 10). The activation of ROS production by that cell is then sensed by the cell following it in the chain, via its own HPCA1, and the process is repeated forming a positive amplification loop that drives the ROS signal from cell-to-cell until all cells in the plant turn their ROS production state to "activated".

While the initiation of the cell-to-cell ROS signal is primarily dependent on RBOHD (Miller et al., 2009; Fichman et al., 2019), its propagation is dependent on HPCA1, RBOHD, and RBOHF (Figure 5), that together could amplify the ROS signal (Figure 10). CIPK26 can activate RBOHF and OST1 (Drerup et al., 2013; Mogami et al., 2015), while OST1 can activate RBOHD and RBOHF (Sirichandra et al., 2009; Wang et al., 2020; Figures 7–10). Activation of HPCA1 could also cause the opening of aquaporins such as PIP2;1 (Rodrigues et al., 2017; Smirnoff and Arnaud, 2019; Maurel et al., 2021; Mittler et al., 2022) and facilitate the transfer of RBOH-generated ROS into cells. The enhanced production of apoplastic ROS by each cell could therefore alter the ROS and redox state of the cytosol (Fichman and Mittler, 2021b), in an aquaporin- and plasmodesmata-dependent manner (Fichman et al., 2021), and activate multiple transcriptional regulators such as MYB30 and ZAT12 (Figure 4; Fichman et al., 2020; Mittler et al., 2022), causing all cells "excited" or "activated" by the cell-to-cell ROS signal to acquire a heightened state of tolerance to the stress and become acclimated (Figures 4, 7, 9, and 10; Zandalinas et al., 2020a, 2020b; Fichman et al., 2021; Fichman and Mittler, 2021b; Mittler et al., 2022). Cell-to-cell ROS signaling therefore plays a key role in plant acclimation to stress, and HPCA1 is a key component of this pathway enabling ROS sensing and continued signal propagation (Figure 10).

Materials and methods

Plant material, growth conditions, and generation of transgenic plants

Arabidopsis thaliana Col-0 WT plants, homozygous knockout lines (Alonso et al., 2003) of *hpca1* (AT5G49760; CS923304), *cbl4* (AT5G24270; CS859749; Yang et al., 2019), *cipk26* (AT5G21326; SALK_074944C; Lyzenga et al., 2013), *ost1* (AT4G33950; SALK_020604), *msl3* (AT1G58200; SALK_201695C; CS69719), *rbohD* (AT5G47910; CS68747; Torres et al., 2002), and *rbohF* (AT1G64060; CS68748; Torres

et al., 2002), as well as native promoter complementation lines of *rbohD* with full-length genomic sequence of *RBOHD*, *RBOHD* S22–26A, *RBOHD* S22–26–343–347A (Nühse et al., 2007), cDNA sequence of *RBOHD* (Zandalinas et al., 2020b), and cDNA sequence of *RBOHD* without its RD (ΔM1-S347; generated as described below) were used for the main figures (additional mutants are described in Supplemental Table S1). Plants were grown in peat pellets (Jiffy International, Kristiansand, Norway) under controlled conditions of 10-h/14-h light/dark regime, 50 μmol photons s^{-1} m^{-2} (provided by F40T12/DX/ALTO—40 Watt Fluorescent Tube Daylight-6500K; Philips, Andover, MA, USA) and 21°C for 4 weeks (Zandalinas et al., 2020a, 2020b; Fichman et al., 2021).

For constructing RBOHD without the RD (ΔM1-S347), a DNA fragment lacking the *RbohD* RD (from amino acids 348–921) was amplified by polymerase chain reaction (PCR) from cDNA template (using specific primers:

5′-GAGACTCGAGATGCAGAAGCTTAGACCGGCAAA-3′

and 5′-TCTCGAGCTCCTAGAAGTTCTCTTTGTGGAAGT-3′), isolated and sequenced. The resulting *RBOHD* sequence without its RD was cloned into pCAMBIA2301 vectors (Marker Gene Technologies, Eugene, OR, USA) downstream of the native *RBOHD* promoter (Nühse et al., 2007; Zandalinas et al., 2020b) replacing the full-length cDNA sequence of *RBOHD* (using XhoI and SacI). *Agrobacterium tumefaciens* GV3101 (Koncz and Schell, 1986) was transformed with the binary plasmid and transgenic Arabidopsis plants were generated using floral dipping (Clough and Bent, 1998). Transformed seedlings were selected on 0.5× Murashige and Skoog media plates (Caisson Labs, Smithfield, UT, USA) supplemented with 50 μg mL^{-1} Kanamycin (Gold Bio, St. Louis, MO, USA) for three generations. Transgenic double homozygous *pZAT12:Luc rbohD* plants (Miller et al., 2009; Zandalinas et al., 2020b) were also complemented with the different *RBOHD* constructs (i.e. full-length genomic sequence of *RBOHD*, *RBOHD* S22–26A, *RBOHD* S22–26–343–347A, cDNA sequence of *RBOHD*, and *RBOHD* ΔM1-S347) as described above.

Grafting

Grafting was performed as previously described (Fichman et al., 2021). Briefly, Arabidopsis plants (WT and different mutants) were germinated on 0.5× Murashige and Skoog media plates (Caisson Labs, Smithfield, UT, USA). An incision was made in 7-day-old stock seedlings to insert a scion into the cut while keeping the rosette of the stock plant intact. Plants were grown for five days in growth chamber at 20°C under constant light. Surviving grafted plants were transplanted to peat pellets and grown as described above for 5 days before light stress treatment (applied to a single leaf of the stock). For each knockout line, four combinations were constructed and tested: WT as the scion and the stock, the mutant line as the scion and the stock, mutant scion on WT stock, and WT scion on a mutant stock. Grafting was repeated 40 times for each combination of each line with ∼40% success rate.

Stress application, imaging of ROS, calcium and membrane potential, and H_2O_2 quantification

As previously described (Fichman et al., 2019; Zandalinas et al., 2020b; Fichman and Mittler, 2021a; Supplemental Figure S4), plants were fumigated for 30 min with 50-μM H_2DCFDA (Millipore-Sigma, St. Louis, MO, USA) for ROS imaging (Fichman et al., 2019; Zandalinas et al., 2020b), 4.5-μM Fluo-4-AM (Becton, Dickinson and Company, Franklin Lakes, NJ, USA) for calcium imaging (Fichman and Mittler, 2021a), 20-μM $DiBAC_4(3)$ (Biotium, Fermont, CA, USA) for membrane potential imaging (Fichman and Mittler, 2021a), or 100-μM PO1 (Millipore-Sigma, St. Louis, MO, USA) for H_2O_2 imaging (Fichman et al., 2019), using a nebulizer (Punasi Direct, Hong Kong, China) in a glass container. Following fumigation, different stresses were applied as described in Fichman et al. (2019); Zandalinas et al. (2020b); Fichman and Mittler (2021a). Briefly, plants were subjected to HL stress by illuminating a single leaf with 1,700-μmol photons $s^{-1}m^{-2}$ using a ColdVision fiber optic LED light source (Schott, Southbridge, MA, USA; Fichman et al., 2019; Zandalinas et al., 2020b); pathogen infection was performed by dipping a single leaf in a solution containing H_2DCFDA and 10^6 CFU of *Pseudomonas syringae* DC 3000 or the same solution without the bacteria (mock; Fichman et al., 2019); for wounding, a single leaf was pierced simultaneously by 20 dress pins (Fichman et al., 2019; Fichman and Mittler, 2021a); for salt stress, a single leaf was dipped in 100-mM NaCl, 50-mM phosphate buffer, pH 7.4, with 50-μM H_2DCFDA for 30 s (the same solution without NaCl was used for mock control); for H_2O_2 treatment, a single leaf was dipped in 1-mM H_2O_2, 50-mM phosphate buffer, pH 7.4, with 50-μM H_2DCFDA for 30 s (the same solution without H_2O_2 was used for mock control). Fluorescence images were acquired using IVIS Lumina S5 (PerkinElmer, Waltham, MA, USA) for 30 min. ROS, H_2O_2, and calcium accumulation, as well as membrane depolarization were analyzed using Living Image 4.7.2 software (PerkinElmer, Waltham, MA, USA) using the math tools (Fichman et al., 2019; Zandalinas et al., 2020b; Fichman and Mittler, 2021a). Time course images were generated and radiant efficiency of regions of interest were calculated. Each data set includes standard error of 8–12 technical repeats. Please note that due to the high sensitivity of this method, background ROS levels are occasionally detected in vascular and meristematic tissues of control untreated plants (Fichman et al., 2019).

Hydrogen peroxide quantification was performed with Amplex-Red (10-Acetyl-3,7-dihydroxyphenoxazine; ADHP; Thermo Fisher Scientific, Waltham, MA, USA). Local and systemic leaves from the different treatments were flash frozen in liquid nitrogen, ground to fine powder, resuspended in 50 μL 0.1-M trichloroacetic acid (TCA; Thermo Fisher Scientific, Waltham, MA, USA), and centrifuged for 15 min at 12,000*g*, 4°C. The supernatant was buffered with 1-M phosphate buffer pH 7.4, and the pellet was dried and used for dry weight calculation. H_2O_2 quantification at the supernatant was performed according to the MyQubit-Amplex-Red Peroxide Assay manual (Thermo Fisher Scientific, Waltham,

MA, USA), using a calibration curve of H_2O_2 (Thermo Fisher Scientific, Waltham, MA, USA). In short, 100 µL of the working solution (100 µM ADHP, 0.02 U horseradish peroxide in reaction buffer) was mixed with 100 µL of the sample. After 30 min of incubation in dark, 20 µL from the reaction was diluted in 180 µL of reaction buffer and fluorescence was measured with a Qubit 4 (Thermo Fisher Scientific, Waltham, MA, USA), using the peroxide protocol. Concentration values were normalized to dry weight of each sample.

Systemic acquired acclimation and electrolyte leakage assays

Local and systemic acquired acclimation to HL stress were measured by subjecting a local leaf to light stress (1,700 µmol photons $s^{-1}m^{-2}$) for 0 or 10 min, incubating the plant under controlled conditions for 50 min, and then exposing the same leaf (local) or a younger leaf (systemic) to HL stress (1,700 µmol photons $s^{-1}m^{-2}$) for 45 min (Zandalinas et al., 2020b; Fichman et al., 2021). Electrolyte leakage was measured by immersing the sampled (treated, untreated, local, or systemic) leaf in distilled water for 1 h and measuring the conductivity of the water using Oakton CON 700 conductivity meter (Thermo Fisher Scientific, Vernon Hills, IL, USA). Samples were then boiled with the water, cooled down to room temperature, and measured again for conductivity (total leakage). Electrolyte leakage was calculated as percentage of the conductivity before heating the samples over that of the boiled samples and compared between plants treated for 10 min on local leaf (pretreated) or treated for 0 min on their local leaf (non-pretreated). Experiments consisted of five repeats for each condition in each line. Standard error was calculated using Microsoft Excel; one-way ANOVA (Analysis of variance; confidence interval = 0.05) and Tukey honestly significant difference (HSD) were performed with IBM SPSS 25.

Transcript expression

Transcript expression in response to HL stress in local and systemic leaves was measured using 4-week-old WT and *hpca1-1* plants following the application of HL to a single leaf for 2 min (Fichman et al., 2021; Fichman and Mittler, 2021a). Exposed leaf (local) and unexposed fully developed younger leaf (systemic) were collected for RNA extraction at 0- and 30 min. RNA was extracted using Plant RNeasy kit (Qiagen, Hilden, Germany) according to the manufacture instructions. Total RNA was used for cDNA synthesis (PrimeScript RT Reagent Kit; Takara Bio, Takara Bio, Kusatsu, Japan). Transcript expression was quantified by real-time qPCR using iQ SYBR Green supermix (Bio-Rad Laboratories, Hercules, CA, USA), as previously described (Fichman et al., 2021; Fichman and Mittler, 2021a), with the following primers:

APX2 (AT3G09640) 5′-TCATCCTGGTAGACTGGACAAA-3′ and 5′-CACATCTCTTAGATGATCCACACC-3′;

MYB30 (AT3G28910) 5′-CCACTTGGCGAAAAAGGCTC-3′ and 5′- ACCCGCTAGCTGAGGAAGTA-3′;

ZAT10 (AT1G27730) 5′-ACTAGCCACGTTAGCAGTAGC-3′ and 5′- GTTGAAGTTTGACCGGAAGTC-3′;

ZAT12 (AT5G59820) 5′-TGGGAAGAGAGTGGCTTGTTT-3′ and 5′- TAAACTGTTCTTCCAAGCTCCA-3′;

ZHD5 (AT1G75240) 5′-CCACCAATCCAAGTCTCCCTC-3′ and 5′-GCTCGCCGCATGATTCTTTAG-3′ and

ELONGATION FACTOR 1 ALPHA (5′-GAGCCCAAGTTTTTGAAGA-3′ and 5′-TAAACTGTTCTTCCAAGCTCCA-3′) was used for normalization of relative transcript levels. Results in the exponent of base 2 delta–delta terminal cycle were obtained by normalizing the relative transcript and comparing it to control WT from local leaf. Data represent 12 biological repeats and 3 technical repeats for each reaction. Standard error and Student *t* test were calculated with Microsoft Excel.

ZAT12 promoter activity

Expression of luciferase driven by the *ZAT12* promoter was detected by luminescence imaging (Miller et al., 2009; Zandalinas et al., 2020b). Plants were sprayed with 1-mM luciferin (Gold Bio, St. Louis, MO, USA), and a single leaf was exposed to HL stress for 2 min (1,700 µmol photons s^{-1} m^{-2}; ColdVision fiber optic LED light source; Schott, Southbridge, MA, USA). Plants were then imaged with the IVIS Lumina S5 apparatus (PerkinElmer, Waltham, MA, USA), as described before (Zandalinas et al., 2020b). Results are presented as precent of control (0 min). Each data set includes standard error of 8–12 technical repeats.

Statistical analysis

All experiments were repeated at least three times with at least three biological repeats. Graphs were generated with Microsoft Excel and are box plots with *X* as mean ± SE. *P*-values ($^*P < 0.05$, $^{**}P < 0.01$, $^{***}P < 0.001$) were generated with two-tailed Student *t* test paired samples. ANOVA followed by a Tukey's HSD post hoc test was used for hypothesis testing (different letters denote statistical significance at $P < 0.05$; Supplemental Data Set 2).

Accession numbers

HPCA1: AT5G49760, *APX2*: AT3G09640, *CBL4*: AT5G24270, *CIPK26*: AT5G21326, *MYB30*: AT3G28910, *OST1*: AT4G33950, *MSL3*: AT1G58200, *RBOHD*: AT5G47910, *RBOHF*: AT1G64060, *ZAT10*: AT1G27730, *ZAT12*: AT5G59820, *ZHD5*: AT1G75240.

Data and materials availability

All data and materials are available upon request from RM (mittlerr@missouri.edu).

Supplemental data

The following materials are available in the online version of this article.

Supplemental Figure S1. MSL3 is required for systemic cell-to-cell calcium signaling in response to hydrogen peroxide.

Supplemental Figure S2. RBOHD is required for systemic cell-to-cell ROS signal initiation and propagation, while RBOHF is required for systemic signal propagation.

Supplemental Figure S3. HPCA1 or MSL3 are not required for systemic cell-to-cell calcium responses to salt stress.

Supplemental Figure S4. Imaging of ROS, calcium, and membrane potential in WT plants subjected to a HL stress treatment applied to a single leaf.

Supplemental Data Set 1. List of mutants that were screened for the presence or absence of the systemic ROS wave in response to a local highlight stress applied to a single leaf.

Supplemental Data Set 2. Data on statistical analysis.

Acknowledgments

We thank The Arabidopsis Biological Resource Center (ABRC), and Professors E.E. Farmer, S. Karpinski, E. Liscum, C. Maurel, S. Pandey, A. S. Richter, G. Stacey and S. Zhang for seeds that were used for the screens shown in Supplemental Data Set 1.

Funding

National Science Foundation grants IOS-2110017, IOS-1932639; Interdisciplinary Plant Group, University of Missouri.

Conflict of interest statement. None declared.

References

Aguirre J and Lambeth JD. (2010) Nox enzymes from fungus to fly to fish and what they tell us about Nox function in mammals. Free Radic Biol Med **49**: 1342–1353

Alonso J M, Stepanova A N, Leisse TJ, Kim C J, Chen H, Shinn P, Stevenson DK, Zimmerman J, Barajas P, Cheuk R, et al. (2003) Genome-wide insertional mutagenesis of *Arabidopsis thaliana*. Science **301**: 653–657

Clough SJ, Bent AF (1998) Floral dip: a simplified method for Agrobacterium-mediated transformation of *Arabidopsis thaliana*. Plant J **16**: 735–743

Devireddy AR, Liscum E, Mittler R (2020) Phytochrome B is required for systemic stomatal responses and reactive oxygen species signaling during light stress. Plant Physiol **184**: 1563–1572

Dickinson MS, Lu J, Gupta M, Marten I, Hedrich R, Stroud RM (2022) Molecular basis of multistep voltage activation in plant two-pore channel 1. Proc Natl Acad Sci USA **119**: e2110936119

Drerup MM, Schlücking K, Hashimoto K, Manishankar P, Steinhorst L, Kuchitsu K, Kudla J (2013) The calcineurin B-like calcium sensors CBL1 and CBL9 together with their interacting protein kinase CIPK26 regulate the Arabidopsis NADPH oxidase RBOHF. Mol Plant **6**: 559–569

Evans MJ, Choi WG, Gilroy S, Morris RJ (2016) A ROS-assisted calcium wave dependent on the AtRBOHD NADPH oxidase and TPC1 cation channel propagates the systemic response to salt stress. Plant Physiol **171**: 1771–1784

Farmer EE, Gao YQ, Lenzoni G, Wolfender JL, Wu Q (2020) Wound- and mechanostimulated electrical signals control hormone responses. New Phytol **227**: 1037–1050

Fichman Y, Miller G, Mittler R (2019) Whole-plant live imaging of reactive oxygen species. Mol Plant **12**: 1203–1210

Fichman Y, Mittler R (2020a) Rapid systemic signaling during abiotic and biotic stresses: Is the ROS wave master of all trades? Plant J **102**: 887–896

Fichman Y, Mittler R (2020b) Noninvasive live ROS imaging of whole plants grown in soil. Trends Plant Sci **25**: 1052–1053

Fichman Y, Mittler R (2021a) Integration of electric, calcium, reactive oxygen species and hydraulic signals during rapid systemic signaling in plants. Plant J **107**: 7–20

Fichman Y, Mittler R (2021b) A systemic whole-plant change in redox levels accompanies the rapid systemic response to wounding. Plant Physiol **186**: 4–8

Fichman Y, Myers RJ, Grant DG, Mittler R (2021) Plasmodesmata-localized proteins and ROS orchestrate light-induced rapid systemic signaling in Arabidopsis. Sci Signal **14**: eabf0322

Fichman Y, Xiong H, Sengupta S, Azad RK, Hibberd JM, Liscum E, Mittler R (2022) Phytochrome B regulates reactive oxygen signaling during abiotic and biotic stress in plants. bioRxiv 2021.11.29.470478, doi: https://doi.org/10.1101/2021.11.29.470478

Fichman Y, Zandalinas SI, Sengupta S, Burks D, Myers RJ Jr, Azad RK, Mittler R (2020) MYB30 orchestrates systemic reactive oxygen signaling and plant acclimation. Plant Physiol **184**: 666–675

Gutteridge JMC, Halliwell B (2018) Mini-review: Oxidative stress, redox stress or redox success? Biochem Biophys Res Commun **502**: 183–186

Hörandl E, Speijer D (2018) How oxygen gave rise to eukaryotic sex. Proc Royal Soc B **285**: 20172706

Iwashita H, Castillo E, Messina MS, Swanson RA, Chang CJ (2021) A tandem activity-based sensing and labeling strategy enables imaging of transcellular hydrogen peroxide signaling. Proc Natl Acad Sci USA **118**: e2018513118

Jabłońska J, Tawfik DS (2021) The evolution of oxygen-utilizing enzymes suggests early biosphere oxygenation. Nat Ecol Evol **5**: 442–448

Johns S, Hagihara T, Toyota M, Gilroy S (2021) The fast and the furious: rapid long-range signaling in plants. Plant Physiol **185**: 694–706

Karpinski S, Reynolds H, Karpinska B, Wingsle G, Creissen G, Mullineaux P (1999) Systemic signaling and acclimation in response to excess excitation energy in Arabidopsis. Science **284**: 654–657

Koncz C, Schell J (1986) The promoter of TL-DNA gene 5 controls the tissue-specific expression of chimaeric genes carried by a novel type of Agrobacterium binary vector. Mol Gen Genet **204**: 383–396

Kromdijk J, Głowacka K, Leonelli L, Gabilly ST, Iwai M, Niyogi KK, Long SP (2016) Improving photosynthesis and crop productivity by accelerating recovery from photoprotection. Science **354**: 857–861

Laohavisit A, Wakatake T, Ishihama N, Mulvey H, Takizawa K, Suzuki T, Shirasu K (2020) Quinone perception in plants via leucine-rich-repeat receptor-like kinases. Nature **587**: 92–97

Luan S and Wang C (2021) Calcium signaling mechanisms across kingdoms. Annu Rev Cell Dev Biol **37**: 311–340

Lyzenga WJ, Liu H, Schofield A, Muise-Hennessey A, Stone SL (2013) Arabidopsis CIPK26 interacts with KEG, components of the ABA signalling network and is degraded by the ubiquitin–proteasome system. J Exp Bot **64**: 2779–2791

Maurel C, Tournaire-Roux C, Verdoucq L, Santoni V (2021) Hormonal and environmental signaling pathways target membrane water transport. Plant Physiol **187**: 2056–2070

Miller G, Schlauch K, Tam R, Cortes D, Torres MA, Shulaev V, Dangl JL, Mittler R (2009) The plant NADPH oxidase RBOHD

mediates rapid systemic signaling in response to diverse stimuli. Sci Signal **2**: ra45–ra45

Mittler R (2017) ROS are good. Trends Plant Sci **22**: 11–19

Mittler R, Vanderauwera S, Suzuki N, Miller G, Tognetti VB, Vandepoele K, Gollery M, Shulaev V Van Breusegem F (2011) ROS signaling: the new wave? Trends Plant Sci **16**: 300–309

Mittler R, Zandalinas SI, Fichman Y, Van Breusegem F (2022) ROS signalling in plant stress responses. Nat Rev Mol Cell Biol, doi: 10.1038/s41580-022-00499-2 (June 27, 2022)

Mogami J, Fujita Y, Yoshida T, Tsukiori Y, Nakagami H, Nomura Y, Fujiwara T, Nishida S, Yanagisawa S, Ishida T, et al. (2015) Two distinct families of protein kinases are required for plant growth under high external Mg^{2+} concentrations in Arabidopsis. Plant Physiol **167**: 1039–1057

Mousavi SAR, Chauvin A, Pascaud F, Kellenberger S, Farmer EE (2013) Glutamate receptor-like genes mediate leaf-to-leaf wound signalling. Nature **500**: 422–426

Nguyen CT, Kurenda A, Stolz S, Chételat A, Farmer EE (2018) Identification of cell populations necessary for leaf-to-leaf electrical signaling in a wounded plant. Proc Natl Acad Sci USA **115**: 10178–10183

Nühse TS, Bottrill AR, Jones AME, Peck SC (2007) Quantitative phosphoproteomic analysis of plasma membrane proteins reveals regulatory mechanisms of plant innate immune responses. Plant J **51**: 931–940

Ogasawara Y, Kaya H, Hiraoka G, Yumoto F, Kimura S, Kadota Y, Hishinuma H, Senzaki E, Yamagoe S, Nagata K, et al. (2008) Synergistic activation of the Arabidopsis NADPH oxidase AtrbohD by Ca^{2+} and phosphorylation. J Biol Chem **283**:8885–8892

Razzell W, Evans IR, Martin P, Wood W (2013) Calcium flashes orchestrate the wound inflammatory response through DUOX activation and hydrogen peroxide release. Curr Biol **23**: 424–429

Rodrigues O, Reshetnyak G, Grondin A, Saijo Y, Leonhardt N, Maurel C, Verdoucq L (2017) Aquaporins facilitate hydrogen peroxide entry into guard cells to mediate ABA- and pathogen-triggered stomatal closure. Proc Natl Acad Sci USA **114**: 9200–9205

Schieber M, Chandel NS (2014) ROS function in redox signaling and oxidative stress. Curr Biol **24**: R453–R462

Shao Q, Gao Q, Lhamo D, Zhang H, Luan S (2020) Two glutamate- and pH-regulated Ca^{2+} channels are required for systemic wound signaling in Arabidopsis. Sci Signal **13**: aba1453

Sies H, Jones DP (2020) Reactive oxygen species (ROS) as pleiotropic physiological signalling agents. Nat Rev Mol Cell Biol **21**: 363–383

Sirichandra C, Gu D, Hu HC, Davanture M, Lee S, Djaoui M, Valot B, Zivy M, Leung J, Merlot S, et al. (2009) Phosphorylation of the Arabidopsis AtrbohF NADPH oxidase by OST1 protein kinase. FEBS Lett **583**: 2982–2986

Slattery RA, Walker BJ, Weber APM, Ort DR (2018) The impacts of fluctuating light on crop performance. Plant Physiol **176**: 990–1003

Smirnoff N, Arnaud D (2019) Hydrogen peroxide metabolism and functions in plants. New Phytol **221**:1197–1214

Suzuki N, Miller G, Salazar C, Mondal HA, Shulaev E, Cortes DF, Shuman JL, Luo X, Shah J, Schlauch K et al. (2013) Temporal-spatial interaction between reactive oxygen species and abscisic acid regulates rapid systemic acclimation in plants. Plant Cell **25**:3553–3569

Szechynska-Hebda M, Lewandowska M, Witoń D, Fichman Y, Mittler R, Karpinski S (2022) Aboveground plant-to-plant electrical signaling mediates network acquired acclimation. Plant Cell **20**: koac150

Taverne YJ, Merkus D, Bogers AJ, Halliwell B, Duncker DJ, Lyons TW (2018) Reactive oxygen species: Radical factors in the evolution of animal life. BioEssays **40**: 1700158

Torres MA, Dangl JL, Jones JDG (2002) Arabidopsis gp91phox homologues AtrbohD and AtrbohF are required for accumulation of reactive oxygen intermediates in the plant defense response. Proc Natl Acad Sci USA **99**: 517–522

Toyota M, Spencer D, Sawai-Toyota S, Jiaqi W, Zhang T, Koo AJ, Howe GA, Gilroy S (2018) Glutamate triggers long-distance, calcium-based plant defense signaling. Science **361**:1112–1115

Wang P, Hsu CC, Du Y, Zhu P, Zhao C, Fu X, Zhang C, Paez JS, Macho AP, Tao WA, et al. (2020) Mapping proteome-wide targets of protein kinases in plant stress responses. Proc Natl Acad Sci USA **117**: 3270–3280

Waszczak C, Carmody M, Kangasjärvi J (2018) Reactive oxygen species in plant signaling. Annu Rev Plant Biol **69**: 209–236

Wu F, Chi Y, Jiang Z, Xu Y, Xie L, Huang F, Wan D, Ni J, Yuan F, Wu X, et al. (2020) Hydrogen peroxide sensor HPCA1 is an LRR receptor kinase in Arabidopsis. Nature **578**: 577–581

Yang Y, Zhang C, Tang RJ, Xu HX, Lan WZ, Zhao F, Luan S (2019) Calcineurin B-like proteins CBL4 and CBL10 mediate two independent salt tolerance pathways in Arabidopsis. Int J Mol Sci **20**: 2421

Zandalinas SI, Fichman Y, Devireddy AR, Sengupta S, Azad RK, Mittler R (2020a) Systemic signaling during abiotic stress combination in plants. Proc Natl Acad Sci USA **117**: 13810–13820

Zandalinas SI, Fichman Y, Mittler R (2020b) Vascular bundles mediate systemic reactive oxygen signaling during light stress. Plant Cell **32**: 3425–3435

Zheng H, Kim J, Liew M, Yan JK, Herrera O, Bok JW, Kelleher NL, Keller NP, Wang Y (2015) Redox metabolites signal polymicrobial biofilm development via the NapA oxidative stress cascade in Aspergillus. Curr Biol **25**: 29–37

Zhu JK (2016) Abiotic stress signaling and responses in plants. Cell **167**: 313–324